

Semi-Analytic Stellar Structure in Scalar-Tensor Gravity

M.W. Horbatsch¹ and C.P. Burgess^{1,2}

¹ *Dept. of Physics & Astronomy, McMaster University
1280 Main St. W, Hamilton, Ontario, Canada, L8S 4L8.*

² *Perimeter Institute for Theoretical Physics
31 Caroline St. N, Waterloo, Ontario, Canada N2L 2Y5.*

ABSTRACT: Precision tests of gravity can be used to constrain the properties of hypothetical very light scalar fields, but these tests depend crucially on how macroscopic astrophysical objects couple to the new scalar field. We study the equations of stellar structure using scalar-tensor gravity, with the goal of seeing how stellar properties depend on assumptions made about the scalar coupling at a microscopic level. In order to make the study relatively easy for different assumptions about microscopic couplings, we develop quasi-analytic approximate methods for solving the stellar-structure equations rather than simply integrating them numerically. (The approximation involved assumes the dimensionless scalar coupling at the stellar center is weak, and we compare our results with numerical integration in order to establish its domain of validity.) We illustrate these methods by applying them to Brans-Dicke scalars, and their generalization in which the scalar-matter coupling slowly runs – or ‘walks’ – as a function of the scalar field: $a(\phi) \simeq a_s + b_s\phi$. (Such couplings can arise in extra-dimensional applications, for instance.) The four observable parameters that characterize the fields external to a spherically symmetric star are the stellar radius, R , mass, M , scalar ‘charge’, Q , and the scalar’s asymptotic value, ϕ_∞ . These are subject to two relations because of the matching to the interior solution, generalizing the usual mass-radius, $M(R)$, relation of General Relativity. Since ϕ_∞ is common to different stars in a given region (such as a binary pulsar), all quantities can be computed locally in terms of the stellar masses. We identify how these relations depend on the microscopic scalar couplings, agreeing with earlier workers when comparisons are possible. Explicit analytical solutions are obtained for the instructive toy model of constant-density stars, whose properties we compare to more realistic equations of state for neutron star models.

Contents

1. Introduction	1
2. Single-field scalar-tensor models	3
2.1 Action and field equations	3
2.2 Observational constraints	4
2.3 (Quasi) Brans/Dicke scalars	5
3. Stellar structure	5
3.1 Equations of hydrostatic equilibrium	6
3.2 Matching to exterior observables	8
3.3 Stellar structure for quasi-Brans/Dicke scalars	12
3.4 Non-relativistic limit	15
4. Solutions for weak central coupling	18
4.1 The weak-central-coupling expansion	18
4.2 Perturbative relations amongst observables	19
4.3 Non-relativistic polytropes	27
5. Incompressible stars	29
5.1 Incompressible stars with quasi-Brans/Dicke scalars	29
5.2 Perturbative solutions: leading order	30
5.3 Perturbative solutions: next-to-leading corrections	36
5.4 Comparing perturbative solutions with numerics	40
6. Conclusions	41
A. Expansions for large b_s	43

1. Introduction

One way in which candidate quantum theories of gravity can differ from one another is the spectrum of bosons they predict at very low energies. Such fields, if they exist and are sufficiently light, can mediate long-range forces that can observably compete with gravity.

Scalar-tensor theories of gravity are among those that can arise in this way, with light scalar fields in addition to the usual metric tensor [1, 2, 3, 4, 5, 6]. A variety of scalars commonly arise in fundamental theories, although it is very unusual for them to be light

enough to mediate forces over macroscopic distances. They are rarely this light because quantum corrections famously tend to give scalars masses, even if they would have been massless at the purely classical level. But in some circumstances symmetries can protect against masses, such as if the scalar is a pseudo-Goldstone boson [7] for a spontaneously broken approximate symmetry, or part of the low-energy limit of an extra-dimensional model [8].

A good deal of effort has been invested in comparing the predictions of scalar-tensor theories with observations in various astrophysical systems [9, 10, 11, 12, 13, 14, 15, 16, 17], in order to improve the constraints on their existence (or to discover their presence). Binary pulsars are particularly useful for this purpose, since the precision of their timing allows accurate measurements of the relativistic gravitational effects that are generated by the strong gravitational fields present.

Central to these tests is an understanding of how the stellar properties depend on the microscopic couplings of the scalar field to matter. Yet these stellar properties can sometimes be remarkable in scalar-tensor theories in the presence of relativistic sources. In particular a phenomenon called spontaneous scalarization can occur, in which the star above a critical baryonic mass can locally support a scalar field even if the scalar-matter coupling vanishes asymptotically far from the star [18]. This allows scalar-tensor gravity to deviate strongly from General Relativity (GR) near the star while still passing weak-field solar system tests.

Since different fundamental theories predict scalars with different microscopic couplings, it is useful to be able to survey how stellar properties depend on these couplings. For this reason in this paper we re-examine the equilibrium conditions in a star in scalar-tensor models as a function of scalar couplings. In particular we do so working as far as possible within analytic approximation schemes, since these more easily allow the results to be varied for different kinds of scalar properties. We find semi-analytic progress is possible using a weak-coupling approximation for the scalar field near the stellar center. By comparing with numerical integrations of the equations of stellar structure we find the domain of validity of these approximations, which allow us to understand stellar properties fairly well.

As a preliminary to studying the relativistic limit in more detail, we apply our analysis to the special case of an incompressible stellar fluid, for which the energy density is approximately constant. (This can be done consistent with conservation laws only if the pressure is not also regarded as being a function of the energy density.) To leading order in the weak-coupling expansion, the profiles of physical variables of constant-density stars can be described in closed form in terms of elementary functions, dilogarithms, and Heun functions.

Although not physically realistic, solutions with this equation of state can give insight into general features of relativistic stars, in particular near the maximum mass that can be supported by gravitational forces. (For GR the maximum mass found under the assumption of constant density gives an upper bound on the maximum mass that would be found with more realistic equations of state [19].) We compare the predictions of constant density in scalar-tensor theory with those of several representative equations of states for neutron stars.

The rest of the paper is organized as follows. In §2 we define the scalar-tensor theories

of interest, and in particular the parameters describing the couplings of the light scalar to ordinary matter. Following much of the literature we specialize to the case where the scalar-matter couplings are only weakly dependent on the scalar fields themselves — what we call quasi-Brans/Dicke (qBD) models — as well as the constraints on their couplings that are inferred from solar system tests of gravity. §3 then derives the equations describing hydrostatic equilibrium for static and spherically-symmetric stars in scalar-tensor gravity, as well as the matching formulae that relate the interior and exterior geometries. Some of those general properties that can be extracted without solving them explicitly are also discussed, such as whether the pressure need be monotonic; the kinds of relations they imply amongst quantities visible to exterior observers; and the non-relativistic limit. Next, §4 provides a discussion of the perturbative solutions to these equations in the weak-coupling limit, in both the relativistic and non-relativistic cases. The important distinction between perturbations in the strength of the coupling measured at the stellar center, vs its strength at infinity, first arises in this section. Finally, in section §5 the perturbed equations are solved explicitly to leading nontrivial order for the special case of incompressible stars, with the results compared to more realistic equations of state for neutron star models.

2. Single-field scalar-tensor models

We start by defining the field equations of the scalar-tensor systems of interest.

2.1 Action and field equations

We consider a single light scalar field, and choose its action to be given by¹

$$S = -\frac{1}{16\pi G} \int d^4x \sqrt{-g} g^{\mu\nu} (\mathcal{R}_{\mu\nu} + 2 \partial_\mu \phi \partial_\nu \phi) + S_m[\psi, \tilde{g}_{\mu\nu}], \quad (2.1)$$

where a Weyl re-scaling is performed to go to the Einstein frame (which eliminates any ϕ -dependence from the Einstein-Hilbert term) and the scalar field is redefined to ensure its kinetic term is minimal (with a conventional factor of 2). Here G is the Einstein-frame gravitational constant, $g_{\mu\nu}$, is the Einstein-frame metric whose Ricci tensor is $\mathcal{R}_{\mu\nu}$, and S_m denotes the ‘matter’ action, involving all other observed fields (collectively denoted here by ψ).

There are two physical choices made in writing this action, beyond the choice of using only a single scalar field.

- We assume the absence of a scalar potential, which we assume is small enough to be negligible for the astrophysical applications of interest. This would necessarily be true if the scalar is relevant to cosmology, but is also the feature that quantum contributions make most difficult to achieve in realistic models (unless there is an approximate symmetry, like shifts $\phi \rightarrow \phi + c$, for constant c).

¹Conventions: we use metric signature $(-+++)$ and Weinberg’s curvature conventions [20] (differing from MTW [21] only by an overall sign for the Riemann tensor). Units are chosen with $\hbar = c = 1$.

- We assume the matter action, S_m , only depends on ϕ and $g_{\mu\nu}$ through the one ‘Jordan-frame’ combination $\tilde{g}_{\mu\nu} = A^2(\phi)g_{\mu\nu}$, where the conformal factor $A(\phi)$ is a function whose form would be specified within any particular fundamental theory. This kind of coupling actually arises in specific models (such as if ϕ arises as the breathing mode for the geometry of extra dimensions), and has the attractive feature that it naturally evades many of the strongest observational constraints on violations of the equivalence principle.

The field equations obtained by varying (2.1) are

$$\mathcal{R}_{\mu\nu} + 2\partial_\mu\phi\partial_\nu\phi + 8\pi G \left(T_{\mu\nu} - \frac{1}{2}Tg_{\mu\nu} \right) = 0 \quad (2.2)$$

$$\square\phi + 4\pi Ga(\phi)T = 0, \quad (2.3)$$

where $\square = g^{\mu\nu}\nabla_\mu\nabla_\nu$ is the d’Alembertian operator built using the Levi-Civita connection of $g_{\mu\nu}$, while

$$T^{\mu\nu} = -\frac{2}{\sqrt{-g}}\frac{\delta S_m}{\delta g_{\mu\nu}} \quad (2.4)$$

is the Einstein-frame energy-momentum tensor, $T = g^{\mu\nu}T_{\mu\nu}$ is its trace, and $a(\phi) = A'(\phi)/A(\phi)$ defines the scalar-matter coupling function in terms of the function $A(\phi)$.

2.2 Observational constraints

Because it is $\tilde{g}_{\mu\nu}$ that appears in the matter action, it is the geodesic of this Jordan-frame metric along which the trajectories of matter particles tend to move (in the absence of other forces). Upon taking the post-Newtonian limit of the Jordan-frame metric $\tilde{g}_{\mu\nu}$, one finds that the effective Jordan-frame gravitational constant, measured in asymptotic Einstein-frame units,² is

$$\tilde{G} = G \left[1 + a^2(\phi_\infty) \right], \quad (2.5)$$

and that the Jordan-frame parameterized post-Newtonian quantities whose values differ from those of GR are

$$\tilde{\beta} = 1 + \frac{a^2(\phi_\infty)b(\phi_\infty)}{2[1 + a^2(\phi_\infty)]^2}, \quad \tilde{\gamma} = 1 - \frac{2a^2(\phi_\infty)}{1 + a^2(\phi_\infty)}, \quad (2.6)$$

where ϕ_∞ is the asymptotic value of the scalar field far from the source and $b(\phi) = da(\phi)/d\phi$ [2].

Constraints on these PPN parameters from solar system observations provide the best bounds on the model, with $|\tilde{\gamma} - 1| < 2.3 \times 10^{-5}$ inferred from Cassini tracking, and $|\tilde{\beta} - 1| < 2.3 \times 10^{-4}$ from lunar laser ranging [9]. This corresponds to the coupling bounds

$$a^2(\phi_\infty^{SS}) < 1.2 \cdot 10^{-5} \quad \text{and} \quad a^2(\phi_\infty^{SS})|b(\phi_\infty^{SS})| < 4.6 \cdot 10^{-4}, \quad (2.7)$$

where ϕ_∞^{SS} denotes the asymptotic value of ϕ as one leaves the solar system.

²These are units in which the Einstein-frame metric is asymptotically Minkowski: $\text{diag}(-1, 1, 1, 1)$. If one instead uses units in which the Jordan-frame metric is asymptotically Minkowski, then $\tilde{G} = GA^2(\phi_\infty)[1 + a^2(\phi_\infty)]$.

2.3 (Quasi) Brans/Dicke scalars

The simplest scalar-tensor theory is Brans-Dicke theory [22], for which $a(\phi) = a_s$ is constant. In this case – see eq. (2.7) – solar system tests constrain $a_s < 3.5 \cdot 10^{-3}$, and so all of the predictions of Brans-Dicke theory are very close to those of GR.

The next-simplest theory, which we call quasi-Brans/Dicke (qBD) theory, allows $a(\phi)$ to vary slowly with ϕ [23]:

$$A(\phi) = \exp(a_s \phi + \frac{1}{2} b_s \phi^2), \quad a(\phi) = a_s + b_s \phi. \quad (2.8)$$

This introduces a variety of new phenomena because it makes the strength of the scalar-matter couplings depend on ϕ , and so allows them to vary with position and time [24, 25]. This means that couplings in exotic environments (like stellar interiors) could be stronger than naïvely expected without running into conflict with the strong solar-system bounds mentioned above (this is similar in spirit to, but different in detail from, evading these bounds through matter-dependent scalar self-couplings [26, 27, 28]). Assuming ϕ is defined such that $\phi \rightarrow 0$ asymptotically far from the Sun, eqs. (2.7) show that the strong bound on a_s implies that solar system bounds do not strongly constrain b_s .

The constraints on b_s are comparatively weak, and the best come from studies of binary pulsars [29, 30, 31]. The precise timing measurements that are possible for binary pulsars allow their orbits to be accurately measured over long periods of time, and comparing measurements with the predictions of the qBD model leads to the constraint $b_s \gtrsim -5$ [10, 11, 12, 13]. Measurements of the redshift of spectral lines from neutron stars leads to a weaker constraint $b_s \gtrsim -9$ [14]. The main uncertainties in these bounds come from the poor understanding of the nuclear equation of state appropriate for neutron star interiors.

Observations disfavor negative b_s because for $b_s \lesssim -4$, compact objects like neutron stars exhibit a phenomenon called spontaneous scalarization [18]. For sufficiently dense objects, whose precise threshold density depends on b_s and the nuclear equation of state, it is possible for the star to support a nonzero scalar field even though the scalar coupling vanishes asymptotically far from the star: $a(\phi_\infty) = 0$. Furthermore it is known that when scalarization takes place it is the stable solution to the field equations [32, 1]. Scalarized neutron stars tend to be disfavored by binary pulsar observations because scalarization significantly changes the dynamics and radiation generated by a neutron star.

Collapse processes involving scalarized neutron stars have been investigated by a number of authors [33], who found that the waveform of the emitted gravitational radiation depends strongly on b_s . Moreover, scalar-tensor gravity allows monopole and dipole radiation, which are forbidden in GR. Thus, future measurements of gravitational waves may lead to improved constraints on b_s [12].

3. Stellar structure

One of the potential uncertainties when trying to constrain scalar-tensor models using astrophysical tests of gravity is the strength of the scalar field that is supported by objects like

the Sun or a neutron star. For macroscopic astrophysical objects made up of weakly coupled constituents one's intuition is that the scalar coupling to the macroscopic object should be proportional to the scalar coupling to each of its constituents, and we shall see in this section that this intuition is generally borne out for weakly coupled non-relativistic systems. We shall also see that it can fail for relativistic systems, even in the limit of weak scalar coupling.

In order to do so, we next summarize how the scalar field alters the physics of stellar interiors, since it is the matching to this that dictates the properties of the external field configurations to which external observers have observational access.

3.1 Equations of hydrostatic equilibrium

The equations of hydrostatic equilibrium in scalar-tensor gravity were first studied in [34], and subsequently in [35, 36, 37, 38, 39, 40, 41, 42, 43, 44, 45, 46, 18, 47, 48, 49, 50, 51, 52, 53, 54].

Following [18] we model the stellar interior as a static, spherically-symmetric and perfect fluid in local thermal equilibrium, locally characterized (in the Jordan frame) by its pressure, P , and mass-energy density, ρ . Time-independence and spherical symmetry allow the use of Schwarzschild-like coordinates for the Einstein-frame metric interior to the star:

$$g_{\alpha\beta} dx^\alpha dx^\beta = -e^{\nu(r)} dt^2 + \frac{dr^2}{1 - 2\mu(r)} + r^2 d\Omega^2, \quad (3.1)$$

where $d\Omega^2 = d\theta^2 + \sin^2\theta d\phi^2$ denotes the usual round angular metric on the 2-sphere and $\nu(r)$ and $\mu(r)$ are to-be-determined functions that depend only on the radial coordinate r .

The Jordan-frame energy-momentum tensor for matter is defined by

$$\tilde{T}^{\alpha\beta} = -\frac{2}{\sqrt{-\tilde{g}}} \frac{\delta S_m}{\delta \tilde{g}_{\alpha\beta}}, \quad (3.2)$$

and is related to the Einstein-frame energy-momentum tensor by

$$T_{\alpha\beta} = A^2(\phi) \tilde{T}_{\alpha\beta}, \quad T_\alpha{}^\beta = A^4(\phi) \tilde{T}_\alpha{}^\beta \quad \text{and} \quad T^{\alpha\beta} = A^6(\phi) \tilde{T}^{\alpha\beta}, \quad (3.3)$$

where indices on $\tilde{T}_{\alpha\beta}$ are raised and lowered using the Jordan-frame metric, $\tilde{g}_{\alpha\beta}$.

Being a Jordan-frame perfect fluid, the energy-momentum tensor has the form

$$\tilde{T}_{\alpha\beta} = (\rho + P) \tilde{u}_\alpha \tilde{u}_\beta + P \tilde{g}_{\alpha\beta}, \quad (3.4)$$

where $P = P(r)$ and $\rho = \rho(r)$, and \tilde{u}_α is the Jordan-frame 4-velocity of the perfect fluid, given in co-moving coordinates by

$$\tilde{u}_\alpha = e^{\nu/2} A(\phi) \delta_\alpha^t, \quad (3.5)$$

so that $\tilde{g}^{\alpha\beta} \tilde{u}_\alpha \tilde{u}_\beta = -1$.

When writing the field equations it is convenient to scale out a dimensional factor of the central density, $\rho_0 := \rho(0)$, from the density and pressure,

$$p(r) := \frac{P(r)}{\rho_0} \quad \text{and} \quad \varrho(r) := \frac{\rho(r)}{\rho_0}, \quad (3.6)$$

in terms of which the equation of state is specified by writing $\varrho(r) = \varrho[p(r); p_0]$. Here

$$p_0 := \frac{P(0)}{\rho_0} := \frac{P_0}{\rho_0}, \quad (3.7)$$

labels the star's central pressure in the same units, and the p_0 -dependence of $\varrho[p; p_0]$ is meant to emphasize that the functional form of the equation of state, $P(\rho)$, in general changes as one changes the central density. Notice that our notation implies the identity $\varrho(p_0; p_0) = 1$.

With these choices the Einstein field equation, eq. (2.2), in this geometry boils down to the following three conditions:

$$r\mu' + \mu = 4\pi G\rho_0 r^2 A^4(\phi) \varrho(p) + \frac{r^2}{2}(1 - 2\mu)\phi'^2, \quad (3.8)$$

$$p' = -[\varrho(p) + p] \left[\frac{4\pi G\rho_0 r^2 A^4(\phi) p + \mu}{r(1 - 2\mu)} + \frac{r}{2} \phi'^2 + a(\phi)\phi' \right], \quad (3.9)$$

$$\nu' = \frac{8\pi G\rho_0 r^2 A^4(\phi) p + 2\mu}{r(1 - 2\mu)} + r\phi'^2, \quad (3.10)$$

where primes denote derivatives with respect to r . The scalar wave equation, eq. (2.3), similarly becomes

$$\phi'' = \frac{4\pi G\rho_0 A^4(\phi)}{1 - 2\mu} \left[a(\phi)[\varrho(p) - 3p] + r\phi'[\varrho(p) - p] \right] - \frac{2(1 - \mu)}{r(1 - 2\mu)}\phi'. \quad (3.11)$$

These equations are to be integrated subject to the following initial conditions at the centre of the star:

$$\mu(0) = 0, \quad p(0) = p_0, \quad \phi(0) = \phi_0, \quad \phi'(0) = 0. \quad (3.12)$$

Writing eqs. (3.9) and (3.10) as

$$2p' + (p + \varrho) \left[\nu' + 2a(\phi)\phi' \right] = 0, \quad (3.13)$$

and integrating once allows ν to be written in terms of p and ϕ :

$$\nu = -2f(p; p_0) - 2 \ln A(\phi) + \text{const}, \quad (3.14)$$

where

$$f(p; p_0) = \int_{p_0}^p \frac{d\hat{p}}{\hat{p} + \varrho(\hat{p})}. \quad (3.15)$$

Regarding eq. (3.8) as a linear, first-order differential equation for the product $r\mu$, allows it to be solved to obtain

$$\mu = \frac{1}{r} e^{-\int_0^r \tilde{r}\phi'^2 d\tilde{r}} \int_0^r \hat{r}^2 \left[\frac{\phi'^2}{2} + 4\pi G\rho_0 A^4(\phi) \varrho(p) \right] e^{\int_0^{\hat{r}} \tilde{r}\phi'^2 d\tilde{r}} d\hat{r}, \quad (3.16)$$

where the integration constant is chosen such that (3.12) holds. This expression shows that μ is always non-negative. It also shows that $\mu(r)$ should not be interpreted as the mass-energy inside the ball of radius r , unlike in GR.

In principle, eqs. (3.8) through (3.11) can be integrated numerically, starting at $r = 0$ and continuing out to larger r . In practice, this system of equations is singular at $r = 0$, so numerical integration must be started at some small positive $r = r_0$. The initial conditions at r_0 can be obtained from the power series expansions that are dictated by the equations of motion themselves:

$$\begin{aligned}\mu(r) &= \frac{4\pi G\rho_0 A_0^4}{3} r^2 + \mathcal{O}(r^4), \\ p(r) &= p_0 + \frac{2\pi G\rho_0 A_0^4}{3} (p_0 + 1) [a_0^2(3p_0 - 1) - (3p_0 + 1)] r^2 + \mathcal{O}(r^4), \\ \phi(r) &= \phi_0 - \frac{2\pi G\rho_0 A_0^4}{3} a_0(3p_0 - 1) r^2 + \mathcal{O}(r^4),\end{aligned}\tag{3.17}$$

where $A_0 = A(\phi_0)$ and $a_0 = a(\phi_0)$.

3.2 Matching to exterior observables

The integration within the stellar interior continues until eventually the pressure p vanishes. The value $r = R$ where this happens defines the (Schwarzschild coordinate) radius of the star, beyond which the appropriate solution instead solves the ‘matter-vacuum’ field equations with $\rho = P = 0$. Of course, for generic scalar-tensor theories it might happen that p never actually vanishes, since unlike for GR p need not be a monotonically decreasing function. We comment where we can on the stability of these configurations below, although as we shall see they are unlikely to happen sufficiently close to the Brans-Dicke limit and for non-relativistic equations of state.

Exterior solutions

For $r > R$, an exterior solution is required to satisfy the vacuum field equations,

$$\mathcal{R}_{\alpha\beta} + 2\partial_\alpha\phi\partial_\beta\phi = 0 \quad \text{and} \quad \square\phi = 0,\tag{3.18}$$

for which a closed-form static and spherically symmetric solution may be found by taking $\phi = \phi(r)$ and using the metric

$$ds^2 = -e^{2u} dt^2 + e^{-2u} dr^2 + e^{2v} [d\theta^2 + \sin^2\theta d\varphi^2],\tag{3.19}$$

where $u = u(r)$ and $v = v(r)$. The field equations for ϕ , u and v have the following solutions [55]

$$e^{2u} = \left(1 - \frac{\ell}{r}\right)^x, \quad e^{2v} = r^2 \left(1 - \frac{\ell}{r}\right)^{1-x} \quad \text{and} \quad e^{2\phi} = e^{2\phi_\infty} \left(1 - \frac{\ell}{r}\right)^q,\tag{3.20}$$

where the real constants x and q satisfy $x^2 + q^2 = 1$ and are otherwise arbitrary, leaving three free integration constants: x , ℓ and ϕ_∞ .

These three constants are more conveniently rewritten in terms of the large- r limit of the solution when expressed in the original Schwarzschild coordinates,

$$\begin{aligned} ds^2 &= \left(-1 + \frac{2GM}{r} + \dots \right) dt^2 + \dots \\ e^\phi &= e^{\phi_\infty} \left(1 - \frac{GQ}{r} + \dots \right), \end{aligned} \tag{3.21}$$

where M is the system's ADM mass [56] in the Einstein frame and Q defines its 'scalar charge'. For systems where the scalar coupling, $a(\phi)$, is field-dependent, the asymptotic value of the scalar field, ϕ_∞ , may usefully be traded for the asymptotic value of the scalar coupling strength, $a_\infty = a(\phi_\infty)$.

Together with the star's radius, we see that from the point of view of an external observer there are four independent bulk parameters that characterize any such a star in scalar-tensor theory: M , Q , R and ϕ_∞ . These can be calculated in principle as functions of the stellar equation of state by matching the exterior solution to that of the interior at $r = R$, implying that they are functions of the two parameters, ϕ_0 and p_0 , that define the initial conditions of integration at the stellar center, eq. (3.12). One of our main goals is to identify the two relations that must hold amongst the four external parameters (for any given equation of state),

$$\xi_1(R, M, Q, \phi_\infty) = \xi_2(R, M, Q, \phi_\infty) = 0, \tag{3.22}$$

generalizing the familiar mass-radius relation, $R = R(M)$, that expresses the content of stellar structure within GR. The explicit form of these constraints for scalar-tensor models is discussed in section 4.2 below.

Physically, we expect the value of ϕ_∞ to depend on physics external to the star or stellar system of interest, governed by the local properties of the galaxy in which the stars are located. ϕ_∞ could also depend on cosmological time if ϕ is light enough to be evolving over cosmological time intervals. Thus, only one combination of the four parameters M , Q , R and ϕ_∞ can vary in practice from star to star within a specific galactic neighborhood at a given cosmological epoch. In particular, this means that the scalar charge Q and mass M of a star are not independent parameters for any stars within a local neighborhood at a given epoch.

This result greatly simplifies the phenomenological analysis of binary pulsars. Instead of having two independent parameters describing each of the two stars in the binary system, there is in practice only one and so it suffices to describe the observational constraints as a function of the masses of the two stars, just as in GR. In principle the dependence on ϕ_∞ could complicate the combining of the implications of many pulsars that are located far from one another, but a simple estimate shows that ϕ does not vary strongly across the galaxy, so in practice ϕ_∞ can be taken to have a common for all stars in the galaxy. This approximation is implicitly used in refs. [10, 11, 12], when combined data from several binary pulsars are plotted on one theory-space exclusion plot in terms only of the masses of the two components.

To estimate the variance of $\phi(r)$ across the galaxy, we may use the non-relativistic limit for which $g^{\alpha\beta}T_{\alpha\beta} = A^4(\phi)\tilde{g}^{\alpha\beta}\tilde{T}_{\alpha\beta} = A^4(\phi)(3p - \rho) \simeq -A^4(\phi)\rho$ and so

$$\square\phi = \frac{e^{-\nu/2}\sqrt{1-2\mu}}{r^2} \left(e^{\nu/2} r^2 \sqrt{1-2\mu} \phi' \right)' \simeq \frac{1}{r^2} \left(r^2 \phi' \right)' \simeq 4\pi G a(\phi) A^4(\phi) \rho. \quad (3.23)$$

If, on the right-hand-side, we assume $\phi \simeq \phi_g$ to be approximately constant, then $a(\phi)A^4(\phi) \simeq a_g A_g^4$ is also constant. Then the only r -dependence on this side comes from ρ , and we may estimate how large a deviation from constant ϕ is implied by eq. (3.23). For r large enough that ρ is dominated by Dark Matter, the density profile is $\rho \simeq \rho_g (\ell/r)^2$ so that orbital velocities are r -independent: $v_g^2 \simeq GM(r)/r \simeq 4\pi G \rho_g \ell^2$. Then eq. (3.23) implies

$$\phi(r) \simeq \phi(r') + 4\pi G a_g A_g^4 \rho_g \ell^2 \ln \left(\frac{r}{r'} \right) \simeq a_g A_g^4 v_g^2 \ln \left(\frac{r}{r'} \right). \quad (3.24)$$

This is clearly small because it depends only logarithmically on r , and both a_g and v_g are small. See Appendix B of [57] for a related discussion.

Matching at $r = R$

Requiring continuity of the exterior and interior profiles across $r = R$ implies the three external parameters M , Q , and ϕ_∞ must satisfy [18]

$$s := \frac{GM}{R} = \frac{\mathcal{K}}{2\sqrt{1-2\mu_\star}} \exp \left[-\frac{\mathcal{K}}{\mathcal{L}} \operatorname{arctanh} \left(\frac{\mathcal{L}}{\mathcal{J}} \right) \right], \quad (3.25)$$

$$a_A := \frac{Q}{M} = \frac{2R\phi'_\star(1-2\mu_\star)}{\mathcal{K}}, \quad (3.26)$$

$$\phi_\infty = \phi_\star + \frac{2R\phi'_\star(1-2\mu_\star)}{\mathcal{L}} \operatorname{arctanh} \left(\frac{\mathcal{L}}{\mathcal{J}} \right), \quad (3.27)$$

where

$$\mathcal{J} := 2(1-\mu_\star) + R^2\phi_\star'^2(1-2\mu_\star), \quad (3.28)$$

$$\mathcal{K} := 2\mu_\star + R^2\phi_\star'^2(1-2\mu_\star), \quad (3.29)$$

$$\mathcal{L} := \sqrt{4\mu_\star^2 + 4R^2\phi_\star'^2(1-\mu_\star)(1-2\mu_\star) + R^4\phi_\star'^4(1-2\mu_\star)^2}, \quad (3.30)$$

and $\mu_\star := \mu(R)$, $\phi_\star := \phi(R)$, and $\phi'_\star := \phi'(R)$.

It is sometimes useful to decompose the ADM mass as $M = M_B + \Delta M$, where ΔM is the gravitational binding energy and M_B is the baryonic mass, defined by

$$M_B := 4\pi m_0 \int_0^R dr \frac{n A^3(\phi) r^2}{\sqrt{1-2\mu}}, \quad (3.31)$$

where $n(r)$ is the local baryon-number density, and m_b is the average mass of an individual baryon. This baryonic mass can be related to the stellar pressure and density if the star has constant entropy per nucleon, since in this case it follows from energy conservation that

$$\left(\frac{\rho}{n} \right)' + P \left(\frac{1}{n} \right)' = 0. \quad (3.32)$$

This equation can be used to write n in terms of p ,

$$n = n_0 \left[\frac{p + \varrho(p)}{p_0 + 1} \right] e^{-f(p; p_0)}, \quad (3.33)$$

where $n_0 = n(0)$ and $f(p; p_0)$ is defined in equation (3.15). The baryonic mass then becomes

$$M_B = 4\pi m_0 n_0 \int_0^R e^{-f(p)} \left[\frac{p + \varrho(p)}{p_0 + 1} \right] \frac{A^3(\phi) r^2 dr}{\sqrt{1 - 2\mu}}. \quad (3.34)$$

The quantities s and a_A given by the matching equations, (3.25) and (3.26), are in themselves useful because each has a physical interpretation. s is called the self-gravity³, or compactness, of the star and it provides a dimensionless measure of how relativistic its gravitational field is at the stellar surface, $r = R$. For non-relativistic stars $s \ll 1$, and in general relativity $s \leq \frac{4}{9}$ for any star within which the mass-energy density, ρ , is a non-increasing function of r , a result known as Buchdahl's theorem [19].⁴

Similarly, the quantity a_A can often be interpreted as the effective scalar-matter coupling of the star as seen by the observer at infinity. This can be understood by considering the lowest-order non-relativistic interaction energy between two widely separated stars, A and B, [2]:

$$U_{AB} = -\frac{GM_A M_B}{r_{AB}} - \frac{GQ_A Q_B}{r_{AB}} \equiv -\frac{\tilde{G}_{AB} M_A M_B}{r_{AB}}, \quad (3.35)$$

where

$$\tilde{G}_{AB} = G(1 + a_A a_B) \quad (3.36)$$

is the effective Jordan-frame gravitational constant between the two stars, and r_{AB} is the distance between them. All quantities are measured in units in which the Einstein-frame metric is asymptotically Minkowski⁵.

The connection between a_A and the scalar coupling can also be seen in another way. Since in the non-relativistic limit we have $M \simeq M_B$, and since each individual baryon if separated to infinity would microscopically satisfy $q_b/m_b = a_\infty = a(\phi_\infty)$, we expect that for macroscopic non-relativistic systems $Q/M = (Nq_b)/(Nm_b) = a_\infty$ as well, so

$$\lim_{s \rightarrow 0} a_A = a(\phi_\infty) \quad \text{and} \quad \lim_{s \rightarrow 0} \tilde{G}_{AB} = \tilde{G}, \quad (3.37)$$

where \tilde{G} is the Jordan-frame gravitational constant defined in equation (2.5) [2]. We shall see below that the prediction $Q/M = a(\phi_\infty)$ is given by a more detailed matching calculation, where it can be seen to hold independent of the stellar equation of state in the limit of both non-relativistic sources and weak scalar coupling.

³Note that Will [9] uses s to denote the sensitivity of the mass to the gravitational constant, which he defines as $-(\partial \log M)/(\partial \log G)$. This definition of s differs from our definition, but has the same order of magnitude.

⁴The potential generalization of this result to scalar-tensor gravity is investigated in [58].

⁵As mentioned earlier, to convert to units with an asymptotically Minkowski Jordan-frame metric multiply \tilde{G}_{AB} by $A^2(\phi_\infty)$, multiply r_{AB} by $A(\phi_\infty)$, and divide M_A , M_B and U_{AB} by $A(\phi_\infty)$.

The black hole limit

For sufficiently massive stars the only stable configuration in GR is a black hole, for which there is only the exterior solution, eq. (3.20) with $x = 1$ and $q = 0$ [20, 21]. In this case the role of matching to an interior geometry across $r = R$ becomes replaced by the boundary condition that the geometry not have a physical singularity at the event horizon, $r = R_{bh}$, making this the natural equivalent of the stellar radius, R , for a black hole. Since for spherically symmetric stars in GR we have $R_{bh} = 2GM$, we see that for black holes the mass-radius condition predicted is particularly simple: $s = GM/R_{bh} = \frac{1}{2} > \frac{4}{9}$.

For a black hole coupled to scalar fields the exterior solution, (3.20), always has a curvature singularity at $r = \ell$ whenever $q \neq 0$ [2]. This shows that only $q = 0$ describes a legitimate black hole, for which $\phi = \phi_\infty$ is constant and arbitrary (this is unchanged if $a_\infty = a(\phi_\infty) \neq 0$, because there is no matter exterior to the black hole with which to couple). The metric is then given by the Schwarzschild geometry, just as for GR, implying $s = \frac{1}{2}$ and $Q = 0$ (for all ϕ_∞) even when scalars are present. This is a special case of the no-hair theorems, originally formulated for gravity in [59] and extended to scalar fields in [60].

Stability

Once a solution of equations (3.8)-(3.11) is obtained, and the external parameters (3.25)-(3.27) are calculated, it must be checked whether the solution is stable against perturbations. To do this properly requires working with the time-dependent equations of stellar structure. We here instead follow [18, 32, 1] and perform a simplified analysis.

The main idea builds on the observation that (for general relativity) the equations of hydrostatic equilibrium are equivalent to the problem of extremizing M , while keeping M_B fixed [20]. The idea used in [18, 32, 1] is to assume the same is true for scalar-tensor theories (with ϕ_∞ fixed as well as M_B) although we have been unable to prove this so far in scalar-tensor gravity.

For given values of M_B and ϕ_∞ , one generically finds that there can exist multiple stellar configurations with different values of M . This is illustrated by the plot of M_B versus M given in figure 1 for a one-dimensional family of stellar configurations that share a common value for ϕ_∞ . Whenever two or more values of M are obtained for a given ϕ_∞ we take the configuration with the lowest value of M to be stable, and the others to be unstable.

3.3 Stellar structure for quasi-Brans/Dicke scalars

Of course all of the predictions for quantities like Q/M depend in principle on the details of

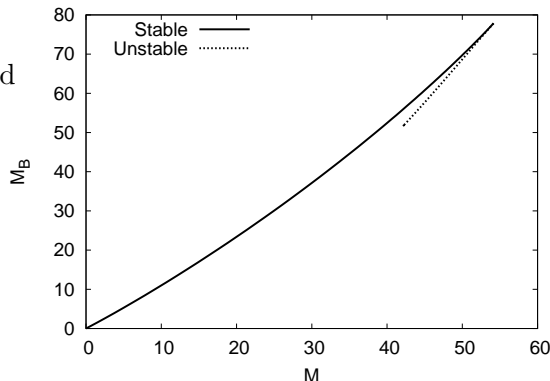


Figure 1: M_B versus M for constant-density stars in Brans-Dicke theory, with $\phi_\infty = 0$ and $a_s^2 = 0.2$.

the coupling function, $a(\phi)$, in addition to depending on the stellar equation of state. In this section we specialize the equations of the previous section to the quasi-Brans/Dicke (qBD) model of eq. (2.8), since this boils the dependence on $a(\phi) = a_s + b_s\phi$ down to the dependence on the two parameters a_s and b_s .

Because the gravity-scalar part of the theory is invariant under constant shifts, $\phi \rightarrow \phi + c$, this transformation can be used to set a_s to zero with no loss of generality, provided that $b_s \neq 0$. With this choice, the matter coupling can be seen to have a reflection symmetry $\phi \rightarrow -\phi$. We henceforth choose this convention for a_s , making it sufficient to follow the dependence of observables on b_s .

Consider now integrating the field equations starting from $r = 0$. The information that used to reside in a_s now resides in the value of the field (or coupling) at the stellar origin, $a_0 := a(\phi_0) = b_s\phi_0$. Suppose first that the initial value, ϕ_0 , chosen for ϕ at the stellar center is such that the coupling vanishes there, $a(\phi_0) = 0$. In this case the reflection symmetry implies $\phi(r) \equiv 0$ for all r is a solution to the field equations, and so $a(\phi) = a_0 = 0$, everywhere within the stellar interior. (That this is a solution can be seen by direct inspection of eq. (3.11).) In this case the equations of stellar structure, (3.8) through (3.11), uniquely reduce to those of GR.

If instead $a_0 = a(\phi_0) = b_s\phi_0 \neq 0$, then, after the change of variables

$$\varphi = (\phi - \phi_0)/a_0, \quad u = 8\pi G\rho_0 A_0^4 r^2, \quad (3.38)$$

the equations of stellar structure simplify to

$$\dot{\mu} = -\frac{\mu}{2u} + \frac{\varrho(p) e^{4a_0^2\varphi(1+b_s\varphi/2)}}{4} + a_0^2 u(1-2\mu)\dot{\varphi}^2, \quad (3.39)$$

$$\dot{p} = -[\varrho(p) + p] \left[\frac{\mu}{2u(1-2\mu)} + \frac{pe^{4a_0^2\varphi(1+b_s\varphi/2)}}{4(1-2\mu)} + a_0^2 \dot{\varphi}(1 + u\dot{\varphi} + b_s\varphi) \right], \quad (3.40)$$

$$\ddot{\varphi} = -\frac{(3-4\mu)\dot{\varphi}}{2u(1-2\mu)} + \frac{e^{4a_0^2\varphi(1+b_s\varphi/2)}}{8u(1-2\mu)} \left[(1+b_s\varphi)[\varrho(p) - 3p] + 2[\varrho(p) - p]u\dot{\varphi} \right], \quad (3.41)$$

where dots denote derivatives with respect to u . These equations show that $a_0 = a(\phi_0) = a(r=0)$ only enters physical observables through its square: a_0^2 . In terms of these variables the initial conditions are

$$\mu(0) = 0, \quad p(0) = p_0, \quad \varphi(0) = 0, \quad \dot{\varphi}(0) = \frac{1}{12}(1-3p_0). \quad (3.42)$$

The profiles $\mu(u)$, $p(u)$ and $\varphi(u)$ obtained by integrating these equations depend only on the three parameters a_0^2 , b_s , p_0 , as well as on the choice of equation of state $\varrho(p)$.

The baryonic mass, eq. (3.34), then becomes

$$\begin{aligned} M_B &= \frac{2\pi m_0 n_0}{(8\pi G\rho_0)^{3/2} A_0^3} \int_0^U du \frac{p + \varrho(p)}{p_0 + 1} e^{-f(p;p_0)} e^{3a_0^2\varphi(1+b_s\varphi/2)} \sqrt{\frac{u}{1-2\mu}}, \\ &:= \frac{2\pi m_0 n_0}{(8\pi G\rho_0)^{3/2} A_0^3} \mathcal{M}(a_0^2, b_s, p_0), \end{aligned} \quad (3.43)$$

where

$$U(a_0^2, b_s, p_0) = 8\pi G\rho_0 A_0^4 R^2 \quad (3.44)$$

is the value $U = u(R)$ corresponding to the boundary of the star. For a given equation of state, U depends only on a_0^2 , b_s and p_0 , because it can be computed by finding the point at which $p(u)$ vanishes.

Note that the quantities \mathcal{J} , \mathcal{K} , and \mathcal{L} , defined in equations (3.28) through (3.30), depend only on $\mu_\star = \mu(U)$ and $R^2\phi'^2(R) = 4a_0^2U^2\dot{\phi}^2(U)$. Therefore, the compactness s — given by equation (3.25) — also depends only on a_0^2 , b_s and p_0 . The matching conditions at the stellar surface, eqs. (3.26) – (3.27), can be re-written using these variables as

$$\frac{\phi_\infty - \phi_0}{a_0} = \varphi(U) + \frac{4U\dot{\phi}(U)(1 - 2\mu_\star)}{\mathcal{L}} \operatorname{arctanh}\left(\frac{\mathcal{L}}{\mathcal{J}}\right) := \mathcal{F}(a_0^2, b_s, p_0), \quad (3.45)$$

and

$$a_A = \frac{Q}{M} = \frac{4a_0 U\dot{\phi}(U)(1 - 2\mu)}{\mathcal{K}} := a_0\mathcal{A}(a_0^2, b_s, p_0), \quad (3.46)$$

which define the quantities \mathcal{F} and \mathcal{A} .

Properties of the pressure profile

This section briefly pauses to investigate whether the pressure, p , decreases monotonically, and whether the equation $p(u) = 0$ must have a solution.

It is clear that (unlike for GR) dP/dr can be positive for sufficiently large couplings and pressures. This follows from evaluating equations (3.40) and (3.42) at the stellar center,

$$\dot{p}(0) = -\frac{1 + p_0}{12} \left[1 + 3p_0 + a_0^2(1 - 3p_0) \right], \quad (3.47)$$

which (for $p_0 \geq 0$) is strictly non-positive unless $p_0 = P_0/\rho_0 > \frac{1}{3}$ and

$$a_0^2 > a_{0\text{crit}}^2 := \frac{3p_0 + 1}{3p_0 - 1}. \quad (3.48)$$

In general, to determine whether the pressure profile is monotonically decreasing everywhere, it is not sufficient to look only at $\dot{p}(0)$. In the qBD theory with $b_s > 0$, it can happen that $\dot{p}(0) > 0$, $\dot{p}(u_\star) = 0$ for some $u_\star > 0$, and $p(U) = 0$ for some $U > u_\star$. Such a star has its maximum pressure in between the centre and the surface. Similarly, if $b_s < 0$, it can happen that $\dot{p}(0) < 0$, $\dot{p}(u_\star) = 0$ for some $u_\star > 0$, $p(u) > 0$ for all $u \geq 0$, and $p(u) \rightarrow \infty$ as $u \rightarrow \infty$. Such a solution describes an object of infinite extent, and seems unphysical.

By contrast, for Brans Dicke theory our numerical calculations suggest that this kind of complicated behaviour does not take place, and the pressure profile $p(u)$ cannot have any local extrema. We have been unable to prove this analytically, but we have shown that if $a_0^2 = a_{0\text{crit}}^2$, then $\Pi(u) = \eta$ for all u , for all equations of state. This constant-pressure solution appears to be the boundary between the solutions with $\dot{p} > 0$, and those with $\dot{p} < 0$. For Brans Dicke theory Salmona [34] has shown that if $p/\rho < 1/3$ everywhere, then p decreases monotonically everywhere.

If we assume that this simple behaviour of the pressure profile in Brans-Dicke theory is correct, then imposing certain requirements on the properties of the solutions of the equations of hydrostatic equilibrium leads to constraints on a_0^2 . If we require that the pressure is decreasing for all p_0 , then it follows that $a_0^2 < 1$.

A more conservative constraint on a_0^2 can be obtained by using some information about the equation of state. For these purposes it suffices to consider only neutron stars, because only these are relativistic enough to have $p_0 > 1/3$. But neutron-star interiors can be modelled as relativistic polytropes [61], with

$$\frac{\rho}{m_b} = n + \frac{\kappa \hat{n}}{\gamma - 1} \left(\frac{n}{\hat{n}}\right)^\gamma \quad \text{and} \quad \frac{P}{m_b} = \kappa \hat{n} \left(\frac{n}{\hat{n}}\right)^\gamma, \quad (3.49)$$

where n is the baryon number density, $\hat{n} = 0.1 \text{ fm}^{-3}$ is a typical nuclear density, $m_b = 1.66 \cdot 10^{-24} \text{ g}$ is the mass of an average baryon, and κ and γ are constants (γ is called the polytropic index). Notice that these choices imply the central density and pressure are related by $\rho_0/m_b = n_0 + \kappa \hat{n} (n_0/\hat{n})^\gamma / (\gamma - 1)$, and so

$$1 = \frac{m_b n_0}{\rho_0} + \frac{p_0}{\gamma - 1}, \quad (3.50)$$

implying the maximum value of p_0 that is possible is $p_0^{\text{max}} = \gamma - 1$. The functions $\varrho(p)$ and $f(p)$ are similarly given by

$$\varrho(p; p_0) = \frac{p}{\gamma - 1} + \left(\frac{p}{p_0}\right)^{1/\gamma} \left(1 - \frac{p_0}{\gamma - 1}\right), \quad (3.51)$$

$$f(p; p_0) = \ln \left[\frac{\gamma - 1 - p_0 + \gamma p (p_0/p)^{1/\gamma}}{(p_0 + 1)(\gamma - 1)} \right]. \quad (3.52)$$

Requiring that the pressure is decreasing for all relativistic polytropes yields the constraint

$$a_0^2 < \frac{3\gamma - 2}{3\gamma - 4}. \quad (3.53)$$

For the neutron-star equations of state EOS II and EOS A of ref. [18], these bounds evaluate to $|a_0| < 1.29$ and $|a_0| < 1.26$, respectively. Although nowhere near as good as the solar system bounds of eqs. (2.7), they are complementary because they apply to the coupling deep within a neutron star interior, and rely only on general considerations, rather than precise observations.

3.4 Non-relativistic limit

In most stars, relativistic effects are negligible, allowing us to take $p = P/\rho_0 \ll 1$ and $\mu \ll 1$.

In this case, the equations of stellar structure, eqs. (3.8) through (3.11), simplify to

$$r\mu' + \mu \simeq 4\pi Gr^2 A^4(\phi)\rho + \frac{r^2\phi'^2}{2}, \quad (3.54)$$

$$P' \simeq -\rho \left[\frac{\mu}{r} + \frac{r\phi'^2}{2} + a(\phi)\phi' \right], \quad (3.55)$$

$$\phi'' \simeq 4\pi GA^4(\phi)\rho \left[a(\phi) + r\phi' \right] - \frac{2\phi'}{r}, \quad (3.56)$$

$$\nu' \simeq \frac{2\mu}{r} + r\phi'^2, \quad (3.57)$$

where the energy density, ρ , is equivalent to the mass density in the non-relativistic limit.

The matching conditions, eqs. (3.25) through (3.27), similarly simplify to

$$\frac{GM}{R} = \mu(R) + \frac{[R\phi'(R)]^2}{2}, \quad (3.58)$$

$$\frac{GQ}{R} = R\phi'(R), \quad (3.59)$$

$$\phi_\infty = \phi(R) + R\phi'(R). \quad (3.60)$$

Notice that these last two matching conditions quite generally imply

$$\phi(R) = \phi_\infty - \frac{GQ}{R}, \quad (3.61)$$

as is appropriate for the non-relativistic limit of the known external solutions.

Newtonian polytropes

The equation of state that is of most interest for Newtonian systems is that of a polytrope,

$$P = K\rho^{1+1/\chi}, \quad (3.62)$$

where χ is the polytropic index (a constant that need not be an integer), and K is a constant. We briefly specialize to this equation of state here for later use in subsequent sections.

Specializing eqs. (3.54) – (3.57) to this equation of state, (3.62), the above equations simplify after changing to dimensionless variables

$$r = r_s w, \quad \rho = \rho_0 \theta^\chi, \quad (3.63)$$

where $\rho_0 = \rho(0)$, and r_s is a length scale that is to be specified later. Then equations (3.54) – (3.57) become

$$\ddot{\phi} = -\frac{2\dot{\phi}}{w} + CA^4(\phi)\theta^\chi \left[a(\phi) + w\dot{\phi} \right] \quad (3.64)$$

$$\frac{d}{dw} \left[\zeta w^2 \dot{\theta} + \frac{1}{2} w^3 \dot{\phi}^2 + w^2 a(\phi) \dot{\phi} \right] = -CA^4(\phi) w^2 \theta^\chi - \frac{w^2}{2} \dot{\phi}^2, \quad (3.65)$$

$$\mu = -w \left[\zeta \dot{\theta} + \frac{w}{2} \dot{\phi}^2 + a(\phi) \dot{\phi} \right], \quad (3.66)$$

where dots now denote d/dw , and the dimensionful parameters are all rolled into the new dimensionless constants,

$$\zeta := K(\chi + 1)\rho_0^{1/\chi}, \quad C := 4\pi Gr_s^2 \rho_0. \quad (3.67)$$

In these variables the initial conditions are

$$\theta(0) = 1, \quad \dot{\theta}(0) = 0, \quad (3.68)$$

$$\text{and} \quad \phi(0) = \phi_0, \quad \dot{\phi}(0) = 0. \quad (3.69)$$

We now specialize to the quasi-Brans/Dicke models of eq. (2.8), for which we had

$$a_0^2 = a^2(\phi_0) = (a_s + b_s \phi_0)^2 \quad \text{and} \quad \varphi = \frac{\phi - \phi_0}{a_0}. \quad (3.70)$$

If we choose

$$r_s = \frac{1}{A_0^2} \sqrt{\frac{\zeta}{4\pi G \rho_0}} = \frac{1}{A_0^2} \sqrt{\frac{K(\chi + 1)}{4\pi G}} \rho_0^{(1-\chi)/2\chi}, \quad (3.71)$$

so that

$$\zeta = CA_0^4, \quad (3.72)$$

then equations (3.64) – (3.66) become

$$-\frac{d}{dw}(w^2 \dot{\theta}) - \frac{a_0^2 b_s}{\zeta} w^2 \dot{\varphi}^2 = w^2 e^{4a_0^2 \varphi(1+b_s \varphi/2)} \theta^\chi \left[1 + a_0^2 (1 + w\dot{\varphi} + b_s \varphi)^2 \right] \quad (3.73)$$

$$\frac{d}{dw}(w^2 \dot{\varphi}) = \zeta w^2 e^{4a_0^2 \varphi(1+b_s \varphi/2)} \theta^\chi (1 + w\dot{\varphi} + b_s \varphi) \quad (3.74)$$

$$\text{and} \quad \mu = -w \left(\zeta \dot{\theta} + \frac{1}{2} a_0^2 w \dot{\varphi}^2 + a_0^2 (1 + b_s \varphi) \dot{\varphi} \right), \quad (3.75)$$

and the initial conditions of eq. (3.68) for φ now are:

$$\varphi(0) = 0, \quad \dot{\varphi}(0) = 0. \quad (3.76)$$

This system implies the solutions have the following power-series expansions near $w = 0$:

$$\theta(w) = 1 - \frac{1}{6}(1 + a_0^2)w^2 + \mathcal{O}(w^4) \quad (3.77)$$

$$\varphi(w) = \frac{\zeta}{6} w^2 + \mathcal{O}(w^4). \quad (3.78)$$

When written in terms of the variables θ , φ , and w , the matching equations, (3.58) – (3.60), become

$$\frac{GM}{R} = -W \left(\zeta \dot{\theta}(W) + a_0^2 [1 + b_s \varphi(W)] \dot{\varphi}(W) \right) \quad (3.79)$$

$$\frac{GQ}{R} = a_0 W \dot{\varphi}(W) \quad (3.80)$$

$$\text{and} \quad \phi_\infty = \phi_0 + a_0 [\varphi(W) + W \dot{\varphi}(W)], \quad (3.81)$$

where $W = w(R) = R/r_s$ denotes the stellar boundary.

4. Solutions for weak central coupling

Most of what is known about the solutions to the equilibrium equations derived above is based on integrating them numerically, revealing several surprising features such as the phenomenon of spontaneous scalarization [18]. But the regime of most practical interest is weak coupling, $a_0^2 \ll 1$, and since interesting phenomena like scalarization are already present in this limit, it is worth exploiting the simplicity of the weak-coupling regime at the outset, both to simplify the numerics required and (in some cases, see below) to allow analytic solutions to be obtained.

Our goal in this section is to systematically expand in powers of the scalar coupling at the stellar centre, $a_0^2 = a^2(\phi_0) = a^2(r = 0) \ll 1$. By comparing these perturbative results with direct numerical integrations, we show that for small a_0^2 their domain of validity typically covers the entire stellar interior.

Our motivation for pursuing the simplifications introduced by this expansion is the ease of generalizing to different kinds of scalar couplings and to different equations of state. However in this paper we confine our attention to the well-studied qBD case, $a(\phi) = a_s + b_s\phi$, in order to better compare with known results.

4.1 The weak-central-coupling expansion

The weak central-coupling expansion is clearest in the case of qBD models, for which the entire coupling function, $a(\phi)$, is determined by the two parameters $a_0 = a(\phi_0)$ and b_s . In this case the weak central-coupling solutions are obtained by expanding the differential equations in powers of a_0^2 . For Brans-Dicke theory ($b_s = 0$) the coupling is constant and known to be small, $a_0^2 = a_s^2 \lesssim 1.2 \times 10^{-5}$.

For qBD theories the lowest-order expansion of the equilibrium equations, (3.39) through (3.41) gives

$$\dot{\mu} + \frac{\mu}{2u} - \frac{\varrho(p)}{4} \simeq a_0^2 \left[\varrho(p)\varphi \left(1 + \frac{b_s\varphi}{2} \right) + u(1 - 2\mu)\dot{\varphi}^2 \right] + \mathcal{O}(a_0^4) \quad (4.1)$$

$$\dot{p} + \frac{[\varrho(p) + p](2\mu + up)}{4u(1 - 2\mu)} \simeq -a_0^2[\varrho(p) + p] \left[\frac{p\varphi(1 + b_s\varphi/2)}{1 - 2\mu} + \dot{\varphi}(1 + u\dot{\varphi} + b_s\varphi) \right] + \mathcal{O}(a_0^4) \quad (4.2)$$

$$\begin{aligned} \ddot{\varphi} + \frac{(3 - 4\mu)\dot{\varphi}}{2u(1 - 2\mu)} - \frac{1}{8u(1 - 2\mu)} \left[(1 + b_s\varphi)[\varrho(p) - 3p] + 2[\varrho(p) - p]u\dot{\varphi} \right] \\ \simeq \frac{a_0^2\varphi(1 + b_s\varphi/2)}{2u(1 - 2\mu)} \left[(1 + b_s\varphi)[\varrho(p) - 3p] + 2[\varrho(p) - p]u\dot{\varphi} \right] + \mathcal{O}(a_0^4), \end{aligned} \quad (4.3)$$

where dots denote derivatives with respect to $u = 8\pi G\rho_0 A_0^4 r^2$. Notice that the leading contribution to the φ equation depends on the self-coupling b_s , even if $a_0^2 \rightarrow 0$. The boundary conditions are as before: $\mu(0) = \varphi_0 = 0$, $p(0) = p_0$ and $\dot{\varphi}(0) = \frac{1}{12}(1 - 3p_0)$ (and so $\dot{\varphi}(0) > 0$ provided $p_0 < \frac{1}{3}$).

We seek interior profiles $\mu(u)$, $p(u)$ and $\varphi(u)$ obtained by integrating these equations subject to the series *ansätze*,

$$\mu(u) = \sum_{i=0}^{\infty} \mu_{(i)}(u) a_0^{2i}, \quad p(u) = \sum_{i=0}^{\infty} p_{(i)}(u) a_0^{2i} \quad \text{and} \quad \varphi(u) = \sum_{i=0}^{\infty} \varphi_{(i)}(u) a_0^{2i}, \quad (4.4)$$

with the leading expressions for $p_0(u)$ and $\mu_0(u)$ agreeing with the results from GR. In particular, because a_0^2 is small, the pressure profile decreases monotonically, ensuring the existence of a solution for R of $p(R) = 0$. Because of the explicit factor of a_0 appearing in the definition $\varphi := (\phi - \phi_0)/a_0$, given a solution for μ , p and φ correct to order a_0^{2k} , we have a solution for ϕ that is valid to order a_0^{2k+1} . Such solutions are obtained explicitly for $k = 0$ and $k = 1$ for incompressible stars in sections 5.2 and 5.3 below.

4.2 Perturbative relations amongst observables

This same a_0^2 expansion is inherited by the expressions relating the external physical parameters, M , R , Q and ϕ_∞ , by virtue of the matching conditions at $r = R$. Although it is difficult to characterize these constraints analytically in the general case, an expansion in powers of $a_0^2 = a^2(\phi_0)$ allows some progress to be made. To this end write

$$\begin{aligned} U(a_0, b_s, p_0) &\simeq U_{(0)}(p_0) + U_{(1)}(b_s, p_0) a_0^2 + \mathcal{O}(a_0^4) \\ \mathcal{F}(a_0, b_s, p_0) &\simeq \mathcal{F}_{(0)}(b_s, p_0) + \mathcal{F}_{(1)}(b_s, p_0) a_0^2 + \mathcal{O}(a_0^4) \\ \mathcal{A}(a_0, b_s, p_0) &\simeq \mathcal{A}_{(0)}(b_s, p_0) + \mathcal{A}_{(1)}(b_s, p_0) a_0^2 + \mathcal{O}(a_0^4) \\ s(a_0, b_s, p_0) &\simeq s_{(0)}(p_0) + s_{(1)}(b_s, p_0) a_0^2 + \mathcal{O}(a_0^4) \\ \mathcal{M}(a_0, b_s, p_0) &\simeq \mathcal{M}_{(0)}(p_0) + \mathcal{M}_{(1)}(b_s, p_0) a_0^2 + \mathcal{O}(a_0^4). \end{aligned} \quad (4.5)$$

where $s = GM/R$, $\mathcal{F} = (\phi_\infty - \phi_0)/a_0$, $\mathcal{A} = Q/Ma_0 = a_A/a_0$ and so on.

We seek two constraints among the four quantities M , Q , R and ϕ_∞ , and it is convenient to write the first of these as a relationship between M , R and ϕ_∞ , and the second as a relationship between $a_A = Q/M$, $s = GM/R$ and $a_\infty = a(\phi_\infty)$. The convenience of this choice comes from the GR limit, for which the first constraint becomes the usual M - R relation, and the second constraint degenerates into something vacuous: $0 = 0$.

An important point about these constraints is that the dependence of observables like M , Q and R (or U) on ϕ_∞ — or $a_\infty = a(\phi_\infty)$ — arises completely through their dependence on $a_0 = a(\phi_0)$. Obtaining this dependence therefore requires a relation between the scalar field at the origin and infinity: $\phi_0(\phi_\infty)$. This is accomplished by using the function \mathcal{F} , whose definition — see eq. (3.45) — states $\phi_\infty = \phi_0 + a_0 \mathcal{F}$, and so

$$A(\phi_\infty) = A(\phi_0) \exp \left[a_0^2 \left(1 + \frac{b_s \mathcal{F}}{2} \right) \mathcal{F} \right], \quad (4.6)$$

$$a(\phi_\infty) = a(\phi_0)(1 + b_s \mathcal{F}). \quad (4.7)$$

It is tempting to ask at this point whether we are working too hard. In particular, since it is a_∞ and not a_0 that directly controls the strengths of interactions that we see, being

asymptotic observers, perhaps we could avoid the exercise of trading a_0 for a_∞ by directly expanding the field equations in powers of a_∞ rather than a_0 . The reason we do not do so — and indeed the point of expanding in powers of a_0 — is that the mapping defined by eq. (4.7) between a_0 and a_∞ is in general not one-to-one. This is the lesson of scalarization, which relies on $a_\infty = 0$ corresponding to *several* choices: $a_0 = 0$ and $a_0 \neq 0$. It is the option of having a second choice that allows the star to support a scalar field ($Q \neq 0$) despite the vanishing of a_∞ . It is the fact that integration of the field equations makes stellar properties single-valued in a_0 that makes this the natural expansion parameter. The existence of several branches to the function $a_0(a_\infty)$ means that stellar properties need not also be analytic in a_∞ . We describe the relevance of this to scalarization in more detail below.

The generalized mass-radius relation

To obtain the leading form of the constraint generalizing the $M(R)$ relation of GR, set $a_0^2 = 0$ in equations (3.39) – (3.40). The result implies that $\mu_{(0)}$ and $p_{(0)}$ do not depend on b_s . Consequently $U_{(0)}(p_0)$, which is defined by $p_{(0)}(U_{(0)}, p_0) = 0$, also cannot depend on b_s — a fact already indicated in eqs. (4.5). The same is then true for the compactness,

$$s(U, \phi_\infty; b_s) = \frac{GM}{R} \simeq s_{(0)}[U_{(0)}, p_0(U_{(0)})] + \mathcal{O}(a_0^2), \quad (4.8)$$

implying this constraint goes over to the GR limit to leading order in a_0^2 , even though the profile for $\varphi(u)$ need not be trivial (for nonzero b_s). Thus is reproduced the usual M vs R (or U) relation of GR.

Figure 2 illustrates how the generalized mass-radius relation depends on a_s in Brans-Dicke theory (*i.e.* $b_s = 0$) for incompressible stars (discussed in more detail in the next section) and relativistic polytrope models of neutron stars. Each curve traces the relationship between M and R as p_0 is varied, beginning at $M = R = 0$ where $p_0 \rightarrow 0$, and terminating at the point where $p_0 \rightarrow p_0^{\max}$. For incompressible stars, p_0^{\max} is infinite. In general relativity, $M \propto R^3$, and the maximum M and R that can be supported against gravitational collapse are attained in the ultra-relativistic limit. However, once the scalar-matter coupling is turned on, the maximum values of M and R are attained at a finite value of p_0 . As a_s increases, the maximum values of M and R decrease.

The equations of state EOS II and EOS A are defined in reference [18]. They are relativistic polytropes, with a maximum central pressure of $p_0^{\max} = \gamma - 1$, where γ is the polytropic index. Their $M - R$ curves are more complicated than those of incompressible stars, and turning on a weak scalar-matter coupling slightly shifts these curves.

Numerically carrying out the stability analysis described in section 3.2 shows that in all cases, the stellar configurations become unstable after the first turning point where $dM/dR = 0$. Thus, the scalar field destabilizes ultra-relativistic incompressible stars.

For non-relativistic systems the matching condition simplifies to eq. (3.58),

$$s_{(0)} = \mu_{(0)}(U_{(0)}; p_0) \ll 1, \quad (4.9)$$

and although numerical methods are usually required to follow the dependence on $p_0(R)$, more explicit statements about the scalar corrections to this relation are possible for specific choices of equation of state. The examples of Newtonian polytropes and incompressible stars are considered more explicitly below.

Scalar-coupling constraint

For a given equation of state the second observable constraint, eq. (3.46), gives an expression for $a_A = Q/M$ in terms of a_0 , b_s and p_0 . Equation (4.7) can be used to relate $a(\phi_\infty)$ with $a(\phi_0)$, and on expansion yields

$$a(\phi_\infty) \simeq (1 + b_s \mathcal{F}_{(0)})a_0 + b_s \mathcal{F}_{(1)}a_0^3 + \mathcal{O}(a_0^5). \quad (4.10)$$

Therefore,

$$a_A = \frac{Q}{M} = a_0 \mathcal{A}(a_0^2, b_s, p_0) \simeq \frac{a(\phi_\infty) \mathcal{A}_{(0)}}{1 + b_s \mathcal{F}_{(0)}} + \mathcal{O}(a_0^3). \quad (4.11)$$

This expression diverges when $1 + b_s \mathcal{F}_{(0)} \rightarrow 0$. In this limit, one must include the $\mathcal{O}(a_0^3)$ terms in order to obtain a meaningful result. This will be described in the section below.

The dependence of a_A/a_0 on s is shown in Figure 3 for several choices of $a_0 = a_s$ in the special case of Brans-Dicke theory ($b_s = 0$), using for illustration an incompressible star equation of state (see §5, below). Each curve can be parametrized by p_0 . The starting point is at $s = 0$, $\mathcal{A} = 1$ when $p_0 \rightarrow 0$, and the endpoint is reached in the limit $p_0 \rightarrow p_0^{\max}$. These curves show that the small- a_0 limit works well in this case even out to very relativistic stars. Notice that a_A is in general smaller than a_0 , with the suppression increasing for more relativistic stars.

Fig. (3) also compares the amount of this suppression for several other choices for the equation of state, indicating that the suppression for relativistic polytropes (more about which later) is under-estimated for incompressible stars, although they all agree in the non-relativistic limit (for which $s_{(0)} \ll 1$), in agreement with intuition.

For incompressible stars a_A eventually becomes negative. As seen in the insert in Fig. (3), this change in sign takes place before the onset of instability, so there exist stable incompressible stars with $a_A < 0$. The scalar interaction between two stars A and B is attractive if $a_A a_B > 0$, and repulsive if $a_A a_B < 0$. If at least one of A , B is an incompressible star, then both cases are possible. However, negative values of a_A are not seen for the more realistic equations of state, although these do approach $a_A = 0$ when extremely relativistic. This should be compared with the corresponding universal result, $Q = 0$, found above for a static, spherically symmetric black hole.

Spontaneous Scalarization

In the above section, the scalar-coupling constraint was expanded in powers of a_0 , and it was found that at leading order, a_A is a single-valued function of a_∞ . In this section, we take the expansion to next order, and demonstrate that a_A becomes a multi-valued function a_∞ . As

a consequence, a_0 and a_A can both be nonzero even when a_∞ vanishes. The phenomenon where Q/M is nonzero even though $a_\infty = 0$ is called spontaneous scalarization. To simplify notation, write

$$a_\infty = d_1 a_0 + d_2 a_0^3 + \mathcal{O}(a_0^5), \quad (4.12)$$

$$a_A = e_1 a_0 + e_2 a_0^3 + \mathcal{O}(a_0^5). \quad (4.13)$$

Dropping terms of order a_0^5 and inverting equation (4.12) yields

$$a_0 = \omega C_+ + \bar{\omega} C_-, \quad (4.14)$$

where

$$C_\pm = \sqrt[3]{\frac{a_\infty}{2d_2} \pm \sqrt{D}}, \quad D = \left(\frac{a_\infty}{2d_2}\right)^2 + \left(\frac{d_1}{3d_2}\right)^3, \quad (4.15)$$

and $\omega = 1, -e^{-i\pi/3}, -e^{i\pi/3}$. Thus,

$$a_A = (\omega C_+ + \bar{\omega} C_-) e_1 + (\omega C_+ + \bar{\omega} C_-)^3 e_2 + \mathcal{O}(a_0^5). \quad (4.16)$$

If $D > 0$, then the $\omega = 1$ solution is real, and the other two solutions are complex. Thus, specification of a_∞ determines a unique stellar configuration.

If $D < 0$, then all solutions are real. Thus, specification of a_∞ determines three stellar configurations.

In the limit $a_\infty \rightarrow 0$, the $\omega = 1$ solution vanishes, and the other two solutions become

$$a_0 = \pm \sqrt{-\frac{d_1}{d_2}}. \quad (4.17)$$

Therefore, whenever the quantity inside the square root is positive, there exist stellar configurations with $a_\infty = 0$ and

$$a_A = \pm \left\{ \left(-\frac{d_1}{d_2}\right)^{1/2} e_1 + \left(-\frac{d_1}{d_2}\right)^{3/2} e_2 \right\} + \mathcal{O}(a_0^5). \quad (4.18)$$

This is precisely the phenomenon of spontaneous scalarization.

The coefficients d_i and e_i are functions of b_s and p_0 , and they also depend on the equation of state. The solution obtained in section 5.2 for incompressible stars can be used to calculate

$$d_1 = \text{HeunG}(\tilde{a}, \tilde{q}; \tilde{\alpha}, \tilde{\beta}, \tilde{\gamma}, \tilde{\delta}; Z) - \frac{1+p_0}{1+3p_0} \log\left(\frac{1+p_0}{1+3p_0}\right) \text{HeunG}'(\tilde{a}, \tilde{q}; \tilde{\alpha}, \tilde{\beta}, \tilde{\gamma}, \tilde{\delta}; Z), \quad (4.19)$$

$$e_1 = \frac{1+p_0}{b_s(1+3p_0)} \text{HeunG}'(\tilde{a}, \tilde{q}; \tilde{\alpha}, \tilde{\beta}, \tilde{\gamma}, \tilde{\delta}; Z), \quad (4.20)$$

where the arguments inside the Heun functions are given in equations (5.34)-(5.35), and $Z = p_0/(3p_0 + 1)$. Note that in the limit $p_0 \rightarrow 0$, we have $d_1 \rightarrow 1$ and $e_1 \rightarrow 1$. In principle, the next coefficients d_2 and e_2 can be calculated using the solution found in section 5.3. However, the resulting expressions are very complicated.

It follows from equation (4.17) that the onset of scalarization implies $d_1 = 0$. Thus, all the points (b_s, p_0) at which scalarization starts can be found by doing a root search of equation (4.19).

In figure (4), equation (4.19) is plotted versus p_0 , for various negative values of b_s . In all cases, d_1 is a convex function of p_0 , with one global minimum. If $b_s \in (-4.329, 0)$, then d_1 never crosses zero, and there is no scalarization. If $b_s \in (-\infty, -4.329)$, then d_1 has two crossings of zero, which correspond to the scalarization which has been extensively studied in the literature.

In figure (5), equation (4.19) is plotted versus p_0 , for various positive values of b_s . In all cases, d_1 is an oscillatory function of p_0 , and there are multiple regions of scalarization. We have verified numerically that scalarization does actually occur when $d_1 < 0$. However, application of the stability criterion of §3.2 shows that these scalarized stars are unstable whenever $b_s > 0$.

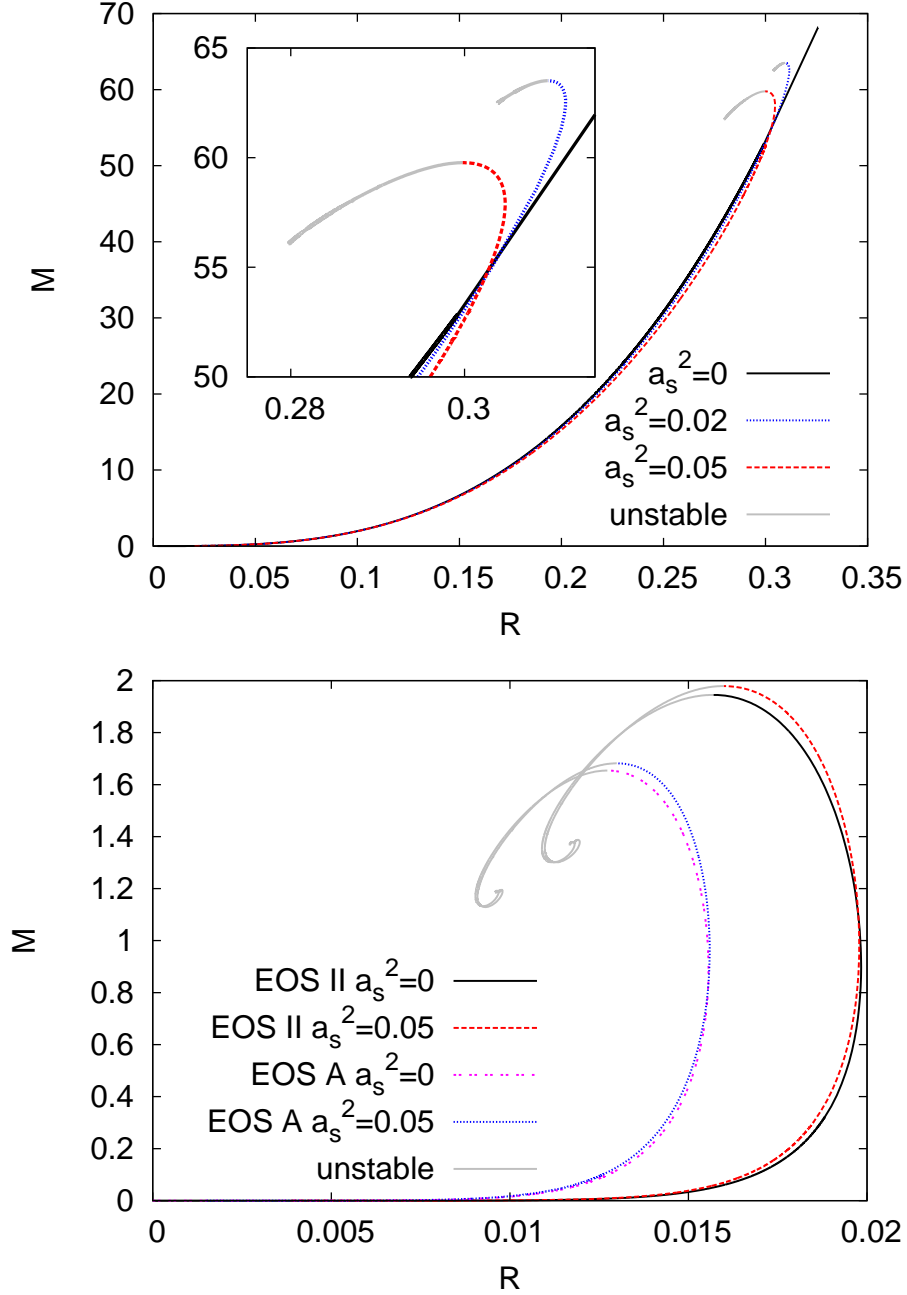


Figure 2: M vs R in Brans-Dicke theory for various equations of state and values of a_s . The central value, $p_0 = P_0/\rho_0$ varies along each curve. The starting point of each curve ($p_0 \rightarrow 0$) is at $M = R = 0$, and the endpoint of each curve corresponds to the ultra-relativistic limit where $p_0 \rightarrow p_0^{\max}$. The values of ϕ_0 are chosen such that ϕ_∞ is constant along each curve. The stellar configurations become unstable after the first turning point where $dM/dR = 0$. Top: Incompressible stars, for which $p_0^{\max} = \infty$. Notice that the curves with non-zero scalar coupling have smaller maximum radii and masses. Bottom: Relativistic polytrope models of neutron stars, as defined in [18], for which p_0^{\max} is finite (colour online).

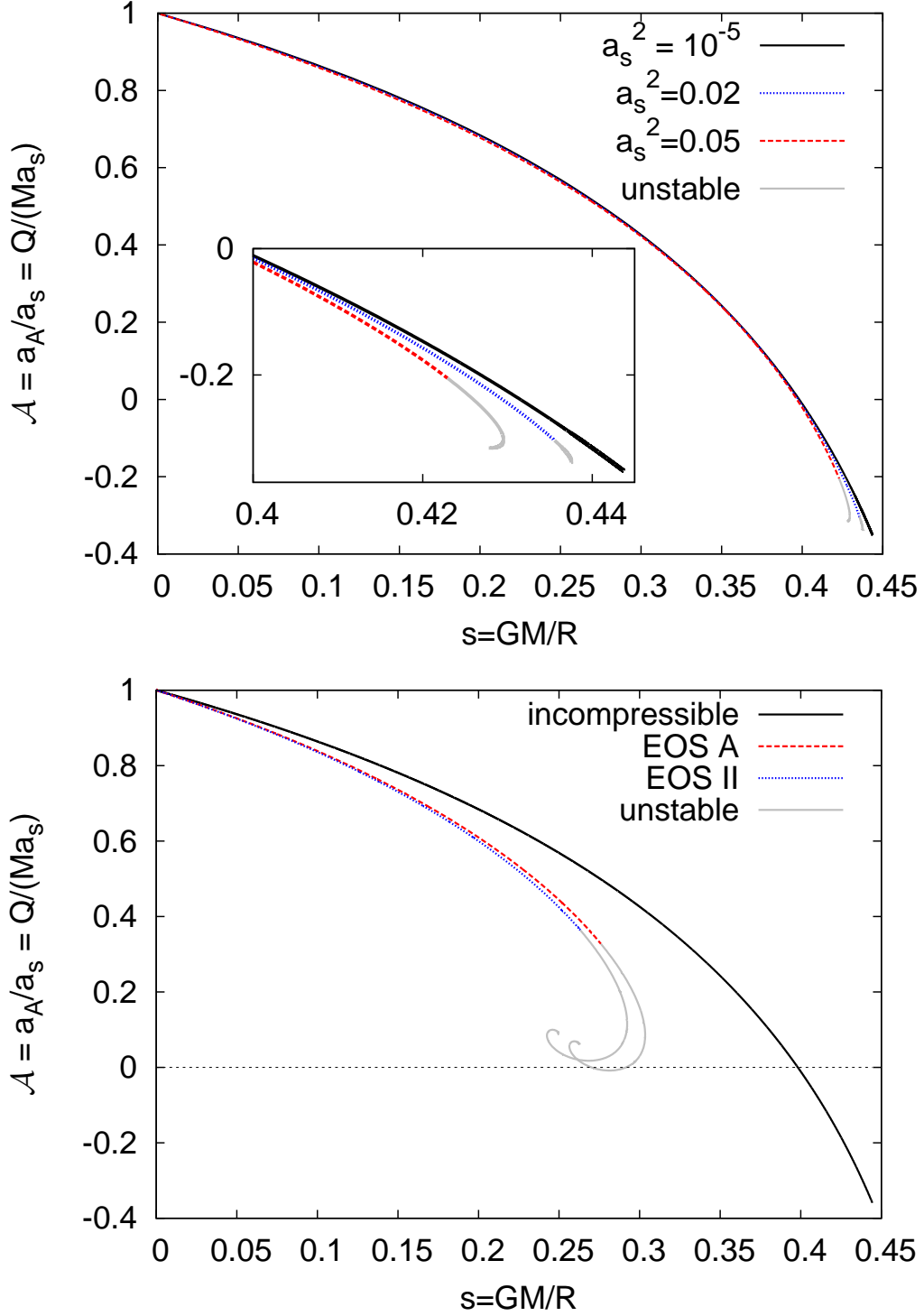


Figure 3: Top: A comparison of $\mathcal{A} = a_A/a_s = Q/(Ma_s)$ vs $s = GM/R$ for incompressible stars in Brans-Dicke theory, for various values of a_s . The curves start at $s = 0$, $\mathcal{A} = 1$ where $p_0 \rightarrow 0$, and terminate where $p_0 \rightarrow \infty$. Bottom: The same quantity comparing incompressible stars with two kinds of neutron-star equations of state (relativistic polytropes) given in [18], using Brans-Dicke theory to leading order in a_s .

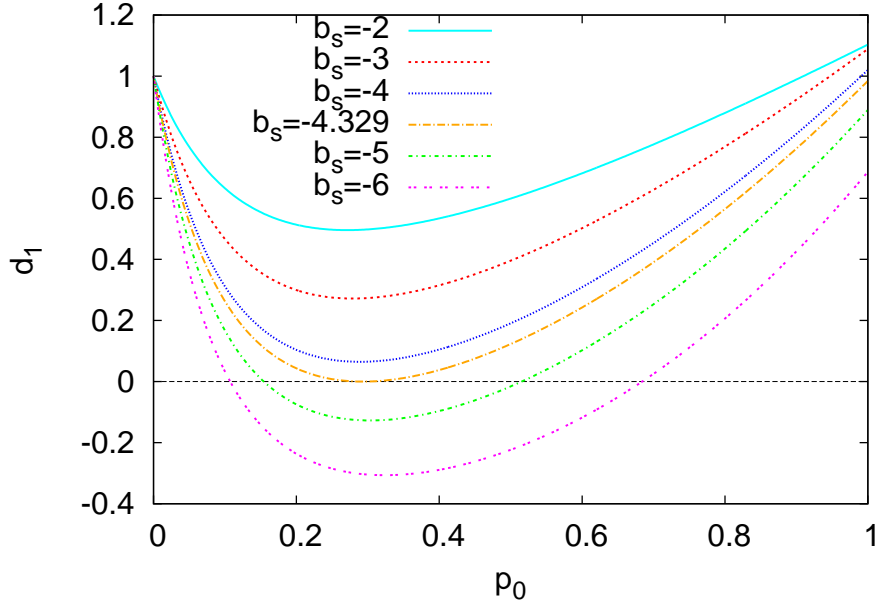


Figure 4: The coefficient d_1 plotted versus p_0 , for constant-density stars, for several choices of $b_s < 0$. Scalarization becomes possible for $b_s < -4.329$.

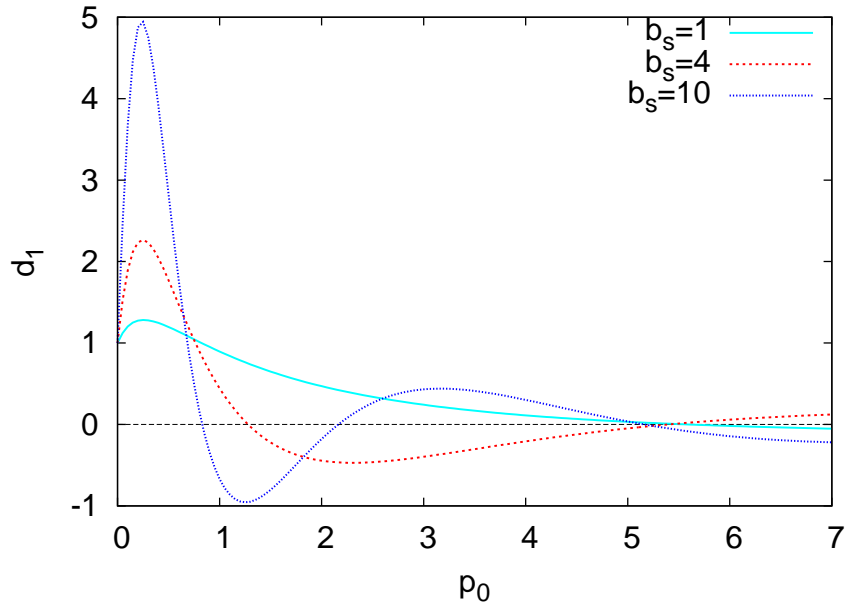


Figure 5: The coefficient d_1 plotted versus p_0 , for constant-density stars, for several choices of $b_s > 0$. There are multiple regions of scalarization.

4.3 Non-relativistic polytropes

As an example for which the scalar-field dependence of the above constraints can be more explicitly explored, consider the case of Newtonian polytropes discussed §3.4 with equation of state $P = K\rho^{1+1/\chi}$. In this case for weak central coupling the scalar field, φ , and the dimensionless density, $\theta = (\rho/\rho_0)^{1/\chi}$, can be expanded in a_0^2 , b_s , as well as the parameter $\zeta = (1 + \chi)K\rho_0^{1/\chi} = (1 + \chi)P_0/\rho_0 = (1 + \chi)p_0$:

$$\theta = \sum_i \theta_{(i)} a_0^{2i} = \sum_{i,j} \theta_{(i,j)} a_0^{2i} b_s^j = \sum_{i,j,k} \theta_{(i,j,k)} a_0^{2i} b_s^j \zeta^k, \quad (4.21)$$

$$\varphi = \sum_i \varphi_{(i)} a_0^{2i} = \sum_{i,j} \varphi_{(i,j)} a_0^{2i} b_s^j = \sum_{i,j,k} \varphi_{(i,j,k)} a_0^{2i} b_s^j \zeta^k. \quad (4.22)$$

We show below that $\zeta \ll 1$ for the polytropes of practical interest, such as white dwarfs and main-sequence stars.

In the limit $a_0^2 = 0$, eqs. (3.73) – (3.74) become

$$\theta'' = -\frac{2\theta'}{w} - \theta^\chi, \quad (4.23)$$

$$\varphi'' = -\frac{2\varphi'}{w} + \zeta\theta^\chi[1 + w\varphi' + b_s\varphi]. \quad (4.24)$$

where for later notational convenience we use primes in this section to denote differentiation with respect to w . Equation (4.23) is called the Lane-Emden equation, and its solutions are well-studied because of its important role in the theory of stellar structure. It can be solved analytically when $\chi = 0, 1, 5$ [64]. The solutions of the Lane-Emden equation with initial conditions (3.68) are called Lane-Emden functions, and are denoted by $\Theta_\chi(w)$. Thus,

$$\theta_{(0)}(w) = \Theta_\chi(w). \quad (4.25)$$

If we now take $b_s = 0$ then equation (4.24) can be solved for φ in terms of θ , giving

$$\varphi'_{(0,0)} = -\frac{\zeta}{w^2} e^{-\zeta(w\Theta_\chi)'} \int^w (\hat{w}^2 \Theta_\chi')' e^{\zeta(\hat{w}\Theta_\chi)'} d\hat{w} \quad (4.26)$$

$$= -\frac{1}{w} + \frac{1}{w^2} e^{-\zeta(w\Theta_\chi)'} \int^w e^{\zeta(\hat{w}\Theta_\chi)'} d\hat{w}. \quad (4.27)$$

Expanding this in powers of ζ then yields

$$\varphi_{(0,0)} \simeq \zeta(1 - \Theta_\chi) + \mathcal{O}(\zeta^2). \quad (4.28)$$

and so

$$\varphi_{(0,0,0)} = 0 \quad \text{and} \quad \varphi_{(0,0,1)} = 1 - \Theta_\chi. \quad (4.29)$$

Expanding the matching equations, eqs. (3.79) – (3.81) in powers of a_0^2 , b_s and ζ similarly yields

$$\frac{GM}{R} \simeq -\zeta W \Theta'_\chi(W) + \mathcal{O}(a_0^2), \quad (4.30)$$

$$\frac{Q}{Ma_0} \simeq 1 + \mathcal{O}(a_0^2) + \mathcal{O}(b_s) + \mathcal{O}(\zeta), \quad (4.31)$$

$$\frac{\phi_\infty - \phi_0}{a_0} \simeq \zeta \left[1 - \Theta_\chi(W) - W \Theta'_\chi(W) \right] + \mathcal{O}(a_0^2) + \mathcal{O}(b_s) + \mathcal{O}(\zeta^2). \quad (4.32)$$

Notice in particular that eq. (4.31) implies that

$$a_A \simeq a_0 \left[1 + \mathcal{O}(a_0^2) + \mathcal{O}(b_s) + \mathcal{O}(\zeta) \right], \quad (4.33)$$

which is consistent with the limit $a_A \rightarrow a(\phi_\infty)$ for weakly self-gravitating stars. Similarly, equation (4.30) can be re-written as

$$\begin{aligned} GM &= -\zeta r_s W^2 \Theta'_\chi + \mathcal{O}(a_0^2) \\ &= -W^2 \Theta'_\chi(W) \left[\frac{\rho_0^{(3-\chi)/2\chi}}{A_0^2} \sqrt{\frac{K^3(\chi+1)^3}{4\pi G}} \right] + \mathcal{O}(a_0^2). \end{aligned} \quad (4.34)$$

which is independent of ρ_0 , as advertised, when $\chi = 3$.

To get an idea about the validity of the ζ expansion, we close this section by estimating its size for the examples of white dwarfs and main-sequence polytropes.

White dwarfs

A white dwarf can be modeled by a degenerate fermion gas which satisfies in the ultra-relativistic limit the polytropic equation of state, eq. (3.62), with

$$K = \frac{3^{1/3} \pi^{2/3}}{4} \left(\frac{Y_e}{m_b} \right)^{4/3} \quad \text{and} \quad \chi = 3. \quad (4.35)$$

Here Y_e is the number of electrons per nucleon and m_b is the average nucleon mass [61]. Although the fermion gas is highly relativistic, the gravitational field generated by it is not strong, allowing use of the non-relativistic expressions developed above.

The typical central densities of white dwarfs are $\rho_0 \sim (10^7 \dots 10^{14}) \text{ kg m}^{-3}$ [61], corresponding to $10^{-5} \lesssim \zeta \lesssim 10^{-2}$ for $Y_e = \frac{1}{2}$. This shows that a perturbative expansion in ζ is likely a good approximation for white dwarfs.

Since the ultra-relativistic limit of the fermion gas is used, the mass calculated below using the matching conditions — *i.e.* equation (4.34) — is greater than the actual mass of the white dwarf. It is instead to be regarded as the Chandrasekhar limit: an upper bound on the mass of white dwarfs. Because $\chi = 3$ its value turns out to be independent of ρ_0 , and for $Y_e = \frac{1}{2}$, its value is approximately $1.4M_\odot$ [62].

Main-sequence models

In the Eddington stellar model, a star is regarded as an ideal gas whose energy is transported by radiation, and it is assumed that the gas makes up a fixed fraction of the total pressure, $\beta := P_{\text{gas}}/P = \text{const.}$ Here P_{gas} is the pressure of the ideal gas, and the total pressure is $P = P_{\text{gas}} + P_{\text{rad}}$, where P_{rad} is the radiation pressure. The Eddington model leads to a polytropic equation of state with

$$K = \left[\frac{45}{\pi^2 k_B^4} \left(\frac{R_g}{\mu} \right)^4 \frac{1 - \beta}{\beta^4} \right]^{1/3} \quad \text{and} \quad \chi = 3, \quad (4.36)$$

where R_g is the universal gas constant, μ is the molar mass of the ideal gas and k_B is Boltzmann's constant [63]. Main-sequence stars can be approximately described by the Eddington standard model, even though convection also plays a role in heat transfer for more realistic models.

For a more accurate single-polytrope model of the Sun, $\chi = 3.35$ and $\zeta \sim 10^{-5}$ [69], so the perturbative expansion in ζ remains a good approximation.

5. Incompressible stars

We now specialize the discussions of the previous sections to the special case of an incompressible star, for which the stellar density, ρ , is constant. Since constant density can only be consistent with the pressure gradients required for hydrostatic equilibrium if $p \neq p(\rho)$, we no longer impose this kind of equation of state. (It is not necessary in any case, since the closure of the field equations is now accomplished by the incompressibility condition, $\rho(r) \equiv \rho_0$.)

The purpose of this exercise is to have a toy example for which all of the above manipulations can be simply carried through explicitly in closed form. Performing the same exercise for GR provides an interesting example that displays the main features of relativistic structure, including the existence of a maximum compactness for a star, $s_{(0)} \leq \frac{4}{9}$, that can be supported against gravitational collapse. The maximum that is found for incompressible stars turns out to provide an upper bound to the maximum compactness that can be achieved with other equations of state.

Several earlier works have numerically investigated incompressible stars in scalar-tensor gravity [36, 40, 45], but our quasi-analytical treatment of these stars is new.

5.1 Incompressible stars with quasi-Brans/Dicke scalars

We cut right to the chase and specialize directly to qBD scalars, for which $a(\phi) = a_s + b_s \phi$, since this case is broad enough to be of wide interest, but restricted enough to be explored in detail.

Field equations

Taking the equation of state to be $\rho = \rho_0$, or $\varrho(p) = 1$, equations (3.39) – (3.41) become

$$\dot{\mu} = -\frac{\mu}{2u} + \frac{1}{4} e^{4a_0^2\varphi(1+b_s\varphi/2)} + a_0^2 u(1-2\mu)\dot{\varphi}^2 \quad (5.1)$$

$$\dot{p} = -(1+p) \left[\frac{\mu}{2u(1-2\mu)} + \frac{p}{4(1-2\mu)} e^{4a_0^2\varphi(1+b_s\varphi/2)} + a_0^2 \dot{\varphi}(1+u\dot{\varphi}+b_s\varphi) \right] \quad (5.2)$$

$$\ddot{\varphi} = -\frac{(3-4\mu)\dot{\varphi}}{2u(1-2\mu)} + \frac{e^{4a_0^2\varphi(1+b_s\varphi/2)}}{8u(1-2\mu)} \left[(1+b_s\varphi)(1-3p) + 2(1-p)u\dot{\varphi} \right]. \quad (5.3)$$

Similarly, the function $f(p)$ defined in eq. (3.15) becomes

$$f(p) = \ln \left(\frac{1+p}{1+p_0} \right), \quad (5.4)$$

and so the baryon number density, $n(r)$, computed from eq. (3.33) is also constant, $n = n_0$. The function \mathcal{M} defined in eq. (3.43) similarly becomes

$$\mathcal{M} = \int_0^U du \sqrt{\frac{u}{1-2\mu}} \exp \left[3a_0^2\varphi \left(1 + \frac{b_s\varphi}{2} \right) \right]. \quad (5.5)$$

5.2 Perturbative solutions: leading order

Because the GR problem can be explicitly integrated for incompressible stars, equations (5.1) – (5.3) can be solved analytically when $a_0^2 = 0$. The zeroth-order profiles, $\mu_{(0)}$ and $p_{(0)}$, are given by [65, 66]

$$\mu_{(0)}(u) = \frac{u}{6}, \quad (5.6)$$

$$p_{(0)}(u) = \frac{(1+3p_0)\sqrt{1-u/3} - (1+p_0)}{3(1+p_0) - (1+3p_0)\sqrt{1-u/3}}, \quad (5.7)$$

as a function of the central pressure p_0 . We return to computing the profile, $\varphi(u)$, below.

At leading order the stellar radius is determined as the zero of $p_{(0)}$, which vanishes at $u = U_{(0)}$ where

$$U_{(0)} = \frac{12p_0(1+2p_0)}{(1+3p_0)^2}, \quad (5.8)$$

corresponding to the radius $r = R_{(0)}$ with

$$R_{(0)} = \frac{2}{A_0^2(1+3p_0)} \sqrt{\frac{3p_0(1+2p_0)}{8\pi G\rho_0}}. \quad (5.9)$$

The leading components of the functions relevant to matching to the exterior solutions — *i.e.* \mathcal{F} , \mathcal{A} , s and \mathcal{M} — are

$$\mathcal{F}_{(0)} = \varphi_{\star(0)} - 12 \left(\frac{1+p_0}{1+3p_0} \right)^2 \ln \left(\frac{1+p_0}{1+3p_0} \right) \dot{\varphi}_{\star(0)}, \quad (5.10)$$

$$\mathcal{A}_{(0)} = 12 \left(\frac{1+p_0}{1+3p_0} \right)^2 \dot{\varphi}_{\star(0)}, \quad (5.11)$$

$$s_{(0)} = \frac{2p_0(1+2p_0)}{(1+3p_0)^2}, \quad (5.12)$$

$$\mathcal{M}_{(0)} = 3\sqrt{3} \left\{ \arccos \left(\frac{1+p_0}{1+3p_0} \right) - 2 \frac{(1+p_0)\sqrt{p_0(1+2p_0)}}{(1+3p_0)^2} \right\}, \quad (5.13)$$

where, as before, the subscript ‘ \star ’ denotes evaluation at $u = U$, so $\varphi_{\star(0)} := \varphi_{(0)}(U_{(0)})$.

Equation (5.12) implies that the compactness is an increasing function of p_0 , which vanishes when $p_0 = 0$ and asymptotes to $\frac{4}{9}$ as $p_0 \rightarrow \infty$. Thus we reproduce the GR result $0 \leq s_{(0)} \leq \frac{4}{9}$ for constant-density stars. This prediction gets modified once $\mathcal{O}(a_0^2)$ corrections are included, however, as is discussed in detail in the next section.

The mass-radius constraint, eq. (4.8), in this case becomes

$$s = \frac{GM}{R} = \frac{4\pi G\rho_0}{3} A_\infty^4 R^2 + \mathcal{O}(a_0^2), \quad (5.14)$$

which states $M \propto R^3$, as might be expected for constant density. This behaviour is seen explicitly in the $a_s = 0$ curve in Fig. (2).

The scalar-coupling constraint, eq. (4.11), similarly becomes

$$a_A = \frac{12a_\infty(1-2s)\dot{\varphi}_{\star(0)}}{1+b_s\varphi_{\star(0)}-6b_s(1-2s)\ln(1-2s)\dot{\varphi}_{\star(0)}} + \mathcal{O}(a_0^3), \quad (5.15)$$

where

$$p_0 = \frac{1-3s-\sqrt{1-2s}}{9s-4} + \mathcal{O}(a_0^2) \quad (5.16)$$

should be substituted into $\varphi_{\star(0)}$ and $\dot{\varphi}_{\star(0)}$ on the right-hand side. Since further progress requires knowing the scalar profile, we next turn to solving its field equation.

Scalar profile in Brans-Dicke theory (when $b_s = 0$)

If $b_s = 0$, then the model reduces to Brans-Dicke theory, and $a(\phi) \equiv a_0 = a_s$. Equation (5.3) with $a_0^2 = 0$ becomes a first-order linear differential equation for $\dot{\varphi}$, which can be solved analytically:

$$\dot{\varphi}_{(0)}(u) = \frac{27(1+p_0) \left(\frac{\arcsin \sqrt{u/3}}{\sqrt{u/3}} - \sqrt{1-u/3} \right) - 4(1+3p_0)u}{12u\sqrt{1-u/3}(3(1+p_0) - (1+3p_0)\sqrt{1-u/3})}. \quad (5.17)$$

Integrating this expression once more with respect to u then gives

$$\begin{aligned} \varphi_{(0)} = & \frac{1}{8(2+3p_0)} \left[(9p_0+5)(3p_0-1) \ln \left(3(1+p_0) - (1+3p_0)\sqrt{1-u/3} \right) \right. \\ & \left. - 9(1+p_0) \left(1+3p_0+3(1+p_0)\sqrt{1-u/3} \right) \frac{\arcsin \sqrt{u/3}}{\sqrt{u/3}} \right] \\ & + \frac{9(1+3p_0)^2(1+p_0)}{16(2+3p_0)^{3/2}} \left[\text{Li}_2(\lambda_-) - \text{Li}_2(\lambda_+) + i \ln \left(\frac{1-\lambda_-}{1-\lambda_+} \right) \arcsin \sqrt{u/3} \right], \end{aligned} \quad (5.18)$$

where

$$\lambda_{\pm} := \frac{(1+3p_0)(\sqrt{1-u/3} + i\sqrt{u/3})}{3(1+p_0) \pm 2\sqrt{2+3p_0}} \equiv |\lambda_{\pm}| e^{i \arcsin \sqrt{u/3}}, \quad (5.19)$$

and

$$\text{Li}_2(z) = \sum_{k=1}^{\infty} \frac{z^k}{k^2} \quad (5.20)$$

is the dilogarithm function.

By using the identity [67]

$$\sum_{k=1}^{\infty} p^k \sin(kx) = \frac{p \sin x}{1 - 2p \cos x + p^2}, \quad (5.21)$$

it can be shown that the imaginary part of (5.18) is constant, and can thus be absorbed into an integration constant. The final normalized and manifestly-real expression for $\varphi_{(0)}$ is then

$$\begin{aligned} \varphi_{(0)}(u) = & \frac{1}{8(2+3p_0)} \left[(9p_0+5)(3p_0-1) \log \left(\frac{3}{2}(1+p_0) - \frac{1}{2}(1+3p_0)\sqrt{1-u/3} \right) \right. \\ & \left. - 9(1+p_0) \left(1+3p_0+3(1+p_0)\sqrt{1-u/3} \right) \frac{\arcsin \sqrt{u/3}}{\sqrt{u/3}} \right] \\ & + \frac{9(1+3p_0)^2(1+p_0)}{16(2+3p_0)^{3/2}} \left[\arctan \left(\frac{2\sqrt{(2+3p_0)u/3}}{1+3p_0-3(1+p_0)\sqrt{1-u/3}} \right) \arcsin \sqrt{u/3} \right. \\ & \left. + \Re [\text{Li}_2(\lambda_-) - \text{Li}_2(|\lambda_-|) - \text{Li}_2(\lambda_+) + \text{Li}_2(|\lambda_+|)] \right] \\ & + \frac{9}{4}(1+p_0). \end{aligned} \quad (5.22)$$

If $p_0 > \frac{1}{\sqrt{3}}$, then the inverse tangent in the above expression changes branch at the critical value

$$u_{\text{crit}} = \frac{4(2+3p_0)}{3(1+p_0)^2} < U_{(0)}, \quad (5.23)$$

so that $\varphi_{(0)}$ is a continuous function of u .

Substituting equation (5.17) into (5.11) yields

$$\mathcal{A}_{(0)} = \frac{9(1+p_0)(1+3p_0)^2}{16[p_0(1+2p_0)]^{3/2}} \arccos \left(\frac{1+p_0}{1+3p_0} \right) - \frac{41p_0^2+34p_0+9}{8p_0(1+2p_0)}, \quad (5.24)$$

so the scalar-coupling constraint, eq. (5.15), can be explicitly evaluated,

$$a_A = a_0 \left(\frac{5}{2} - \frac{9}{4s} - \frac{9\sqrt{1-2s}[27s-14-9\sqrt{1-2s}(2-3s)]}{8[s(5-9s+3\sqrt{1-2s})]^{3/2}} \arccos \sqrt{1-2s} \right) + \mathcal{O}(a_0^3) \quad (5.25)$$

$$= a_0 \left(1 - \frac{6}{5}s + \mathcal{O}(s^2) \right) + \mathcal{O}(a_0^3). \quad (5.26)$$

This confirms that although $a_A \rightarrow a_0$ in the non-relativistic limit $s \rightarrow 0$ — consistent with eq. (3.37) — it is in general depressed relative to a_0 for relativistic systems, even when additional powers of a_0^2 are neglected.

Notice that in the opposite limit we have

$$\lim_{s \rightarrow 4/9} a_A = a_0 \left(\frac{81}{64} \sqrt{2} \arccos(1/3) - \frac{41}{16} \right) + \mathcal{O}(a_0^3) \simeq -0.359a_0 + \mathcal{O}(a_0^3). \quad (5.27)$$

Equation (5.25) is plotted in Figure 3, showing that for incompressible stars a_A passes through zero, changing sign at $s \sim 0.398$. This is compared in the same figure to the corresponding curves for neutron stars modeled by relativistic polytropes, using the equations of state EOS A and EOS II defined in [18]. For small s all three curves agree reasonably well, but differ for large s . For large s the neutron star curves significantly deviate from the constant-density curve, as might be expected given that relativistic polytropes have a maximum value $p_0^{\max} = \gamma - 1$, where γ is the polytropic index, while constant-density stars have no such maximum value for p_0 .

Substituting equations (5.22) and (5.17) into (5.10) yields

$$\begin{aligned} \mathcal{F}_{(0)} = & \frac{9}{4}(1+p_0) - \frac{41p_0^2 + 34p_0 + 9}{8p_0(1+2p_0)} \log(1+3p_0) \\ & + \frac{9(1+p_0)(1+3p_0+3p_0^2)}{4(2+3p_0)\sqrt{p_0(1+2p_0)}} \left(\frac{1+p_0}{\sqrt{p_0(1+2p_0)}} \log(1+p_0) - \arccos \left(\frac{1+p_0}{1+3p_0} \right) \right) \\ & - \frac{9(1+3p_0)^2(1+p_0)}{16(2+3p_0)^{3/2}} \left\{ \arccos \left(\frac{1+p_0}{1+3p_0} \right) \left[\left(\frac{2+3p_0}{p_0(1+2p_0)} \right)^{3/2} \log \left(\frac{1+p_0}{1+3p_0} \right) \right. \right. \\ & \left. \left. + \widetilde{\arctan} \left(\frac{2\sqrt{p_0(1+2p_0)(2+3p_0)}}{1-3p_0^2} \right) \right] \right. \\ & \left. - \Re[\text{Li}_2(\Lambda_-) - \text{Li}_2(|\lambda_-|) - \text{Li}_2(\Lambda_+) + \text{Li}_2(|\lambda_+|)] \right\}, \quad (5.28) \end{aligned}$$

where

$$\Lambda_{\pm} = \frac{1+p_0+2i\sqrt{p_0(1+2p_0)}}{3(1+p_0) \pm 2\sqrt{2+3p_0}} \quad (5.29)$$

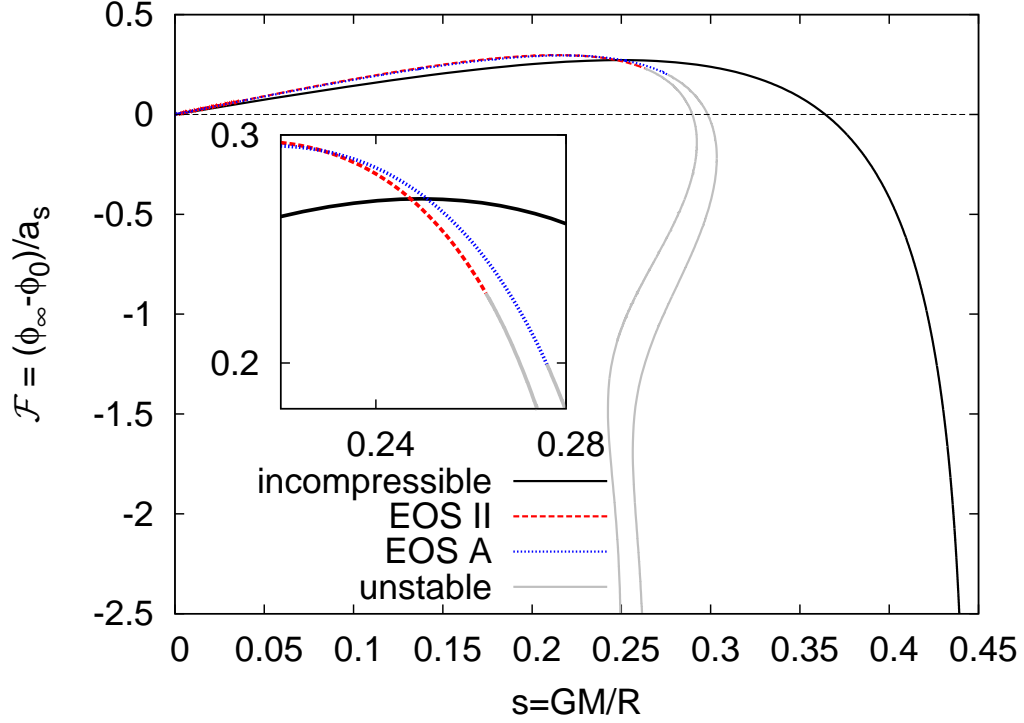


Figure 6: $\mathcal{F} = (\phi_\infty - \phi_0)/a_0$ vs $s = GM/R$ for various stars in Brans-Dicke theory, in the limit $a_0 \rightarrow 0$.

is the value of λ_\pm when $u = U_{(0)}$, and

$$\widetilde{\arctan X} = \begin{cases} \arctan X - \pi & \text{if } 0 < p_0 < \frac{1}{\sqrt{3}}, \\ \arctan X & \text{if } p_0 > \frac{1}{\sqrt{3}}. \end{cases} \quad (5.30)$$

Equation (5.28) is plotted in Figure 6, and is compared to the corresponding curves for neutron stars. Again, the curves are close for small s , and diverge for large s . $\mathcal{F}_{(0)}(s)$ is positive and increasing on the interval $0 < s < 0.25$; positive and decreasing when $0.25 < s < 0.36$; and negative and decreasing for $0.36 < s < \frac{4}{9}$. The maximum value, attained at $s \sim 0.25$, is $\mathcal{F}_{(0),\max} \sim 0.27$. As $s \rightarrow \frac{4}{9}$, $\mathcal{F}_{(0)}$ tends to $-\infty$.

Solution for $b_s \neq 0$

Next suppose $b_s \neq 0$. To calculate $\varphi_{(0)}$, change variables from $(\varphi_{(0)}, u)$ to (ψ, z) with

$$\psi = 1 + b_s \varphi_{(0)}, \quad z = \frac{1}{2} \left(1 - \sqrt{1 - \frac{u}{3}} \right). \quad (5.31)$$

Initial conditions for $\psi(z)$ are then

$$\psi(0) = 1, \quad \left. \frac{d\psi}{dz} \right|_{z=0} = b_s(1 - 3p_0). \quad (5.32)$$

Equation (5.3) with $a_0^2 = 0$ becomes

$$\frac{d^2\psi}{dz^2} + \left(\frac{\tilde{\gamma}}{z} + \frac{\tilde{\delta}}{z-1} + \frac{\tilde{\epsilon}}{z-\tilde{a}} \right) \frac{d\psi}{dz} + \frac{\tilde{\alpha}\tilde{\beta}z - \tilde{q}}{z(z-1)(z-\tilde{a})} \psi = 0, \quad (5.33)$$

where

$$\tilde{a} = -\frac{1}{1+3p_0}, \quad \tilde{q} = \frac{3b_s}{2} \left(\frac{3p_0-1}{3p_0+1} \right), \quad \tilde{\gamma} = \tilde{\delta} = \frac{3}{2}, \quad \tilde{\epsilon} = 1, \quad (5.34)$$

$$\tilde{\alpha} = \frac{3}{2} \left(1 - \sqrt{1 - \frac{8b_s}{3}} \right), \quad \tilde{\beta} = \frac{3}{2} \left(1 + \sqrt{1 - \frac{8b_s}{3}} \right), \quad (5.35)$$

and

$$\tilde{\gamma} + \tilde{\delta} + \tilde{\epsilon} = \tilde{\alpha} + \tilde{\beta} + 1. \quad (5.36)$$

Equation (5.33) is called Heun's equation [68], and is a linear second-order differential equation with singularities at $z = 0, 1, \tilde{a}, \infty$. It is a natural generalization of the hypergeometric equation to the situation having four regular singular points. The solution which satisfies initial conditions (5.32) is the local Frobenius solution about $z = 0$ with exponent 0, and is given by the power series

$$\psi(z) = \text{HeunG}(\tilde{a}, \tilde{q}; \tilde{\alpha}, \tilde{\beta}, \tilde{\gamma}, \tilde{\delta}; z) = \sum_{r=0}^{\infty} c_r z^r, \quad (5.37)$$

where the first two coefficients are given by

$$c_0 = 1, \quad c_1 = \frac{\tilde{q}}{\tilde{a}\tilde{\gamma}}, \quad (5.38)$$

and the higher coefficients are found by solving the three-term recurrence relation

$$\begin{aligned} (r-1+\tilde{\alpha})(r-1+\tilde{\beta}) c_{r-1} \\ - [r(r-1+\tilde{\gamma})(1+\tilde{a}) + r(\tilde{a}\tilde{\delta} + \tilde{\epsilon}) + \tilde{q}] c_r \\ + \tilde{a}(r+1)(r+\tilde{\gamma}) c_{r+1} = 0. \end{aligned} \quad (5.39)$$

In terms of b_s and p_0 , the recursion relation for the coefficients c_r become

$$c_0 = 1, \quad c_1 = b_s(1-3p_0), \quad (5.40)$$

$$\begin{aligned} 2(1+3p_0)(r^2+r-2+6b_s) c_{r-1} \\ - [r(6p_0r+9p_0-1) + 3b_s(3p_0-1)] c_r \\ - (r+1)(2r+3) c_{r+1} = 0. \end{aligned} \quad (5.41)$$

This implies the coefficients c_r of the power series (5.37) can be written explicitly as a polynomial of degree r in b_s ,

$$c_r = \sum_{i=0}^r a_i^{(r)} b_s^i, \quad (5.42)$$

where $a_i^{(r)}$ is itself a polynomial in p_0 of degree r .

The solutions for a_i^r and c_r are found explicitly in the Appendix, where it is also shown that the coefficient of the largest power of b_s has a particularly simple form:

$$a_r^{(r)} = \frac{[6(1-3p_0)]^r}{(2r+1)!}. \quad (5.43)$$

Because b_s is relatively poorly constrained, it can be larger than unity so far as phenomenology is concerned. In this case eq. (5.43) can be used to obtain an approximation for $\varphi(r)$ for large b_s . This gives (see Appendix for details)

$$\begin{aligned} \mathcal{A}_{(0)} &= \frac{1+p_0}{p_0} \left\{ \frac{1}{2b_s} \left(\cosh \sqrt{T} - \frac{\sinh \sqrt{T}}{\sqrt{T}} \right) + \sum_{k=1}^{\infty} \sum_{j=0}^{2k-1} \frac{P_{k,j}(p_0) f_{k,j+1}(T)}{b_s^{k+1} [6(1-3p_0)]^{2k}} \right\}, \quad (5.44) \\ \mathcal{F}_{(0)} &= \frac{1}{b_s} \left(\left[1 + \frac{1+p_0}{2p_0} L \right] \frac{\sinh \sqrt{T}}{\sqrt{T}} - \frac{1+p_0}{2p_0} L \cosh \sqrt{T} - 1 \right) \\ &\quad + \sum_{k=1}^{\infty} \sum_{j=0}^{2k-1} \left(f_{k,j}(T) - \frac{1+p_0}{p_0} L f_{k,j+1}(T) \right) \frac{P_{k,j}(p_0)}{b_s^{k+1} [6(1-3p_0)]^{2k}}, \quad (5.45) \end{aligned}$$

where $T = 6b_s p_0 (1-3p_0) / (1+3p_0)$ and $L = \log(1+p_0) - \log(1+3p_0)$. If $b_s > 0$, then $T \leq (6-4\sqrt{2})b_s \sim 0.34b_s$. If $b_s < 0$, then $T \geq -(6-4\sqrt{2})|b_s| \sim -0.34|b_s|$. The above expressions (5.44) and (5.45) can be used to calculate the second constraint (4.11).

Compactness vs central density

Equation (5.12) describes how the compactness depends on p_0 in GR. In order to find how scalar-matter couplings modify this behaviour, it is necessary to solve the equations of stellar structure to first order in a_0^2 , and calculate $s_{(1)}$.

Figure 7 plots the compactness vs p_0 in Brans-Dicke theory, for various values of the Brans-Dicke coupling $a_0 = a_s$. Notice that the compactness eventually stops growing with p_0 , approaching instead an asymptotic value as $p_0 \rightarrow \infty$. In GR, this asymptotic value is $GM/R = 4/9$, which is the maximum allowed by Buchdahl's theorem. As a_0 increases, this asymptotic value decreases. This is consistent with the results of [40].

5.3 Perturbative solutions: next-to-leading corrections

In this section, $\mathcal{O}(a_0^2)$ corrections are calculated. The defining equation for U is $p(U) = 0$. Expanding it in powers of a_0^2 yields

$$U_{(1)} = \frac{12(1+p_0)^2}{(1+3p_0)^2} p_{(1)}(U_{(0)}). \quad (5.46)$$

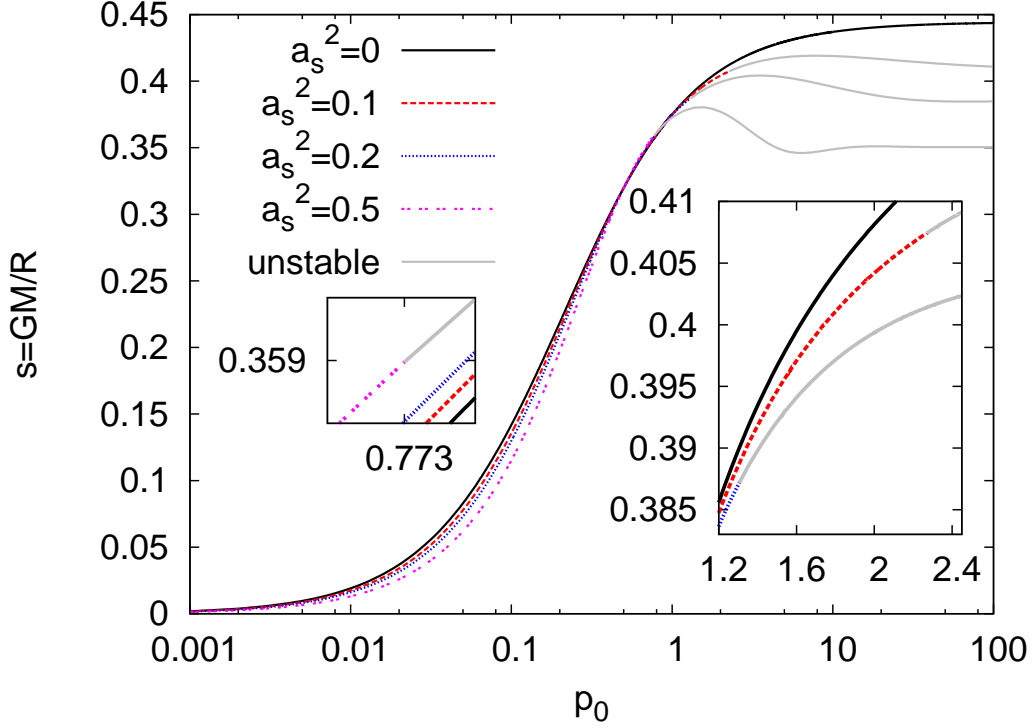


Figure 7: The compactness $s = GM/R$ plotted versus $p_0 = P_0/\rho_0$ for constant-density stars in Brans-Dicke theory, for various values of a_0^2 .

Solving equations (5.1) – (5.3) perturbatively in a_0^2 yields

$$\mu_{(1)}(u) = \frac{1}{\sqrt{u}} \int_0^u d\hat{u} \sqrt{\hat{u}} \left[\varphi_{(0)} \left(1 + \frac{b_s \varphi_{(0)}}{2} \right) + \hat{u}(1 - \hat{u}/3)(\dot{\varphi}_{(0)})^2 \right], \quad (5.47)$$

$$\begin{aligned} p_1(u) &= \frac{2(1+p_0)\varphi_{(0)}(1+b_s\varphi_{(0)}/2)}{(1+3p_0)\sqrt{1-u/3}-3(1+p_0)} \\ &+ \frac{2(1+p_0)\mu_{(1)}(u)}{\sqrt{1-u/3}} \cdot \frac{(1+p_0)(3-2u)\sqrt{1-u/3}-(1+3p_0)}{((1+3p_0)\sqrt{1-u/3}-3(1+p_0))^2} \\ &+ \frac{2(1+p_0)\sqrt{1-u/3}}{6((1+3p_0)\sqrt{1-u/3}-3(1+p_0))^2} \int_0^u \frac{d\hat{u}}{(1-\hat{u}/3)^{3/2}} J(\hat{u}), \end{aligned} \quad (5.48)$$

where the function $J(u)$ appearing in equation (5.48) is given by

$$\begin{aligned} J(u) &= 2 \left[6(1+3p_0)\sqrt{1-u/3} - (1+p_0)(2u^2 - 9u + 18) \right] u(1-u/3)(\dot{\varphi}_{(0)})^2 \\ &- (1+p_0)(4u^2 - 18u + 9)\varphi_{(0)} \left(1 + \frac{b_s \varphi_{(0)}}{2} \right). \end{aligned} \quad (5.49)$$

The perturbation to the scalar profile is similarly

$$\varphi_{(1)} = \Phi_1 \psi + \Phi_2 \tilde{\psi}. \quad (5.50)$$

where the functions ψ and $\tilde{\psi}$ are local Frobenius solutions of equation (5.33) (with parameters (5.34) – (5.35)) about $z = 0$ with exponents 0 and $-\frac{1}{2}$, respectively. They are given by

$$\psi = \text{HeunG}\left(\frac{-1}{1+3p_0}, \frac{3}{2}b_s \cdot \frac{3p_0-1}{3p_0+1}; \frac{3}{2}(1-\sqrt{1-8b_s/3}), \frac{3}{2}(1+\sqrt{1-8b_s/3}), \frac{3}{2}, \frac{3}{2}; z\right), \quad (5.51)$$

$$\tilde{\psi} = \frac{1}{\sqrt{z}} \text{HeunG}\left(\frac{-1}{1+3p_0}, \frac{6b_s(3p_0-1)+1-6p_0}{4(1+3p_0)}; 1 + \frac{3}{2}\sqrt{1-8b_s/3}, 1 - \frac{3}{2}\sqrt{1-8b_s/3}, \frac{1}{2}, \frac{3}{2}; z\right), \quad (5.52)$$

where $z = (1 - \sqrt{1 - u/3})/2$. The coefficients Φ_1 and Φ_2 are given by

$$\Phi_1 = 288 \int_0^z \tilde{\psi}(Fp_{(1)} + G\mu_{(1)} + H)(1-2z)^2[z(1-z)]^{3/2}[1 + (1+3p_0)z] dz, \quad (5.53)$$

$$\Phi_2 = -288 \int_0^z \psi(Fp_{(1)} + G\mu_{(1)} + H)(1-2z)^2[z(1-z)]^{3/2}[1 + (1+3p_0)z] dz, \quad (5.54)$$

where

$$F = -\frac{1 + b_s\varphi_{(0)} + 8z(1-z)\dot{\varphi}_{(0)}}{32z(1-z)(1-2z)^2}, \quad (5.55)$$

$$G = \frac{(4(1+3p_0)z + 1 - 3p_0)(1 + b_s\varphi_{(0)})}{48z(1-z)(1-2z)^4(1 + (1+3p_0)z)} - \frac{[12(1+3p_0)z^3 - 6(1+7p_0)z^2 + (9p_0-5)z + 1]\dot{\varphi}_{(0)}}{12z(1-z)(1-2z)^4(1 + (1+3p_0)z)}, \quad (5.56)$$

$$H = \frac{(4(1+3p_0)z + 1 - 3p_0)\varphi_{(0)}(1 + b_s\varphi_{(0)})(1 + b_s\varphi_{(0)}/2)}{24z(1-z)(1-2z)^2(1 + (1+3p_0)z)} + \frac{(2(1+3p_0)z + 1 - p_0)\varphi_{(0)}(1 + b_s\varphi_{(0)}/2)\dot{\varphi}_{(0)}}{(1-2z)^2(1 + (1+3p_0)z)}. \quad (5.57)$$

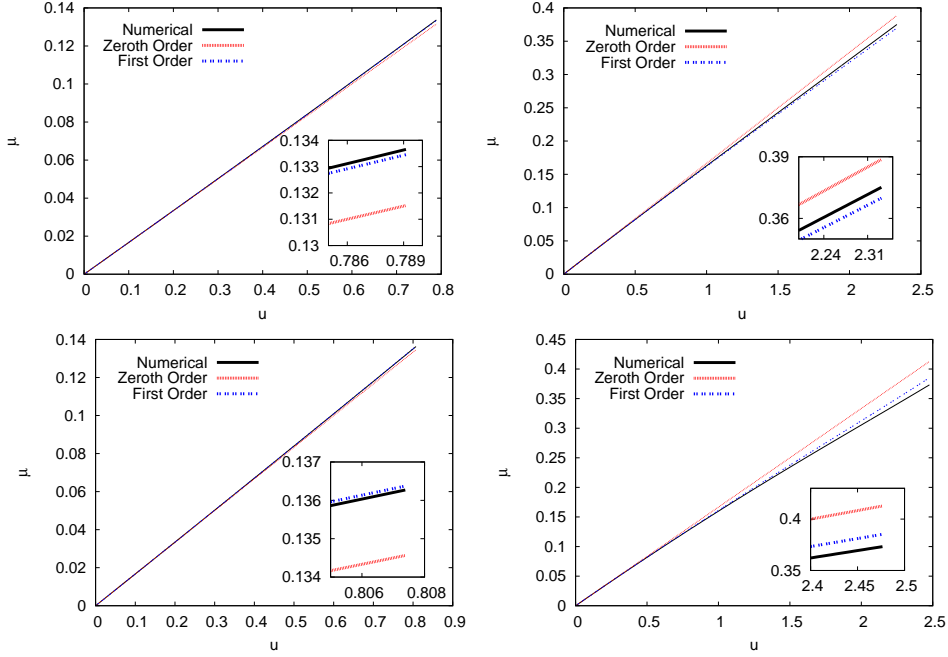


Figure 8: Comparison of μ vs u calculated perturbatively and numerically for an incompressible star in quasi-Brans/Dicke theory with $a_0^2 = 0.1$ and $b_s = 4$, $p_0 = 0.1$ (top left); $b_s = 4$, $p_0 = 1$ (top right); $b_s = -4$, $p_0 = 0.1$ (bottom left); and $b_s = -4$, $p_0 = 1$ (bottom right). All curves terminate at the stellar exterior, $u = U$.

The first-order corrections to the external parameters are given by

$$\begin{aligned}
\mathcal{F}_{(1)} = & \varphi_{(1)} - 12e^{2L}L\dot{\varphi}_{(1)} - \frac{3(1+p_0)^2}{2p_0(1+2p_0)}L(1+b_s\varphi_{(0)})p_{(1)} \\
& + 36e^{2L}\left(1 + \frac{1+4p_0+5p_0^2}{2p_0(1+2p_0)}L\right)\left(p_{(1)}\dot{\varphi}_{(0)} + 48e^{2L}\frac{p_0(1+2p_0)}{(1+3p_0)^2}(\dot{\varphi}_{(0)})^3\right) \\
& + 12\left(1 + \frac{(1+3p_0)^2}{2p_0(1+2p_0)}L\right)\dot{\varphi}_{(0)}\mu_{(1)}, \tag{5.58}
\end{aligned}$$

$$\begin{aligned}
\mathcal{A}_{(1)} = & 12e^{2L}\dot{\varphi}_{(1)} + \frac{3(1+p_0)^2}{2p_0(1+2p_0)}(1+b_s\varphi_{(0)})p_{(1)} - 6\frac{(1+3p_0)^2}{p_0(1+2p_0)}\dot{\varphi}_{(0)}\mu_{(1)} \\
& - 1728e^{4L}\frac{p_0(1+2p_0)}{(1+3p_0)^2}(\dot{\varphi}_{(0)})^3 - 18e^{2L}\frac{(5p_0^2+4p_0+1)}{p_0(1+2p_0)}\dot{\varphi}_{(0)}p_{(1)}, \tag{5.59}
\end{aligned}$$

$$s_{(1)} = \mu_{(1)} + 2e^{2L}p_{(1)} - 144L\frac{p_0(1+2p_0)}{(1+3p_0)^2}e^{4L}(\dot{\varphi}_{(0)})^2, \tag{5.60}$$

$$\begin{aligned}
\mathcal{M}_{(1)} = & \frac{24(1+p_0)\sqrt{3p_0(1+2p_0)}}{(1+3p_0)^2}p_{(1)} + \frac{12\sqrt{3p_0(1+2p_0)}}{1+p_0}\mu_{(1)} \\
& - 3\int_0^{U_{(0)}} du\sqrt{\frac{u}{1-u/3}}[\varphi_{(0)}(1+b_s\varphi_{(0)}/2) + 2u(1-u/3)(\dot{\varphi}_{(0)})^2], \tag{5.61}
\end{aligned}$$

where $L = \log(1+p_0) - \log(1+3p_0)$, and the profiles are all to be evaluated at $U_{(0)}$.

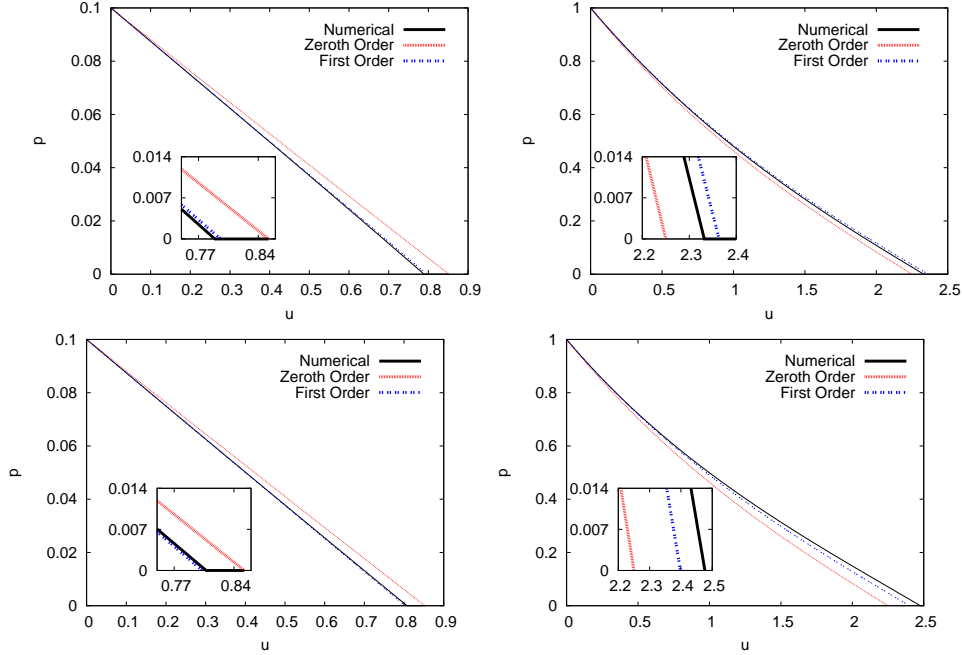


Figure 9: Comparison of p vs u calculated perturbatively and numerically for an incompressible star in quasi-Brans/Dicke theory with $a_0^2 = 0.1$ and $b_s = 4$, $p_0 = 0.1$ (top left); $b_s = 4$, $p_0 = 1$ (top right); $b_s = -4$, $p_0 = 0.1$ (bottom left); and $b_s = -4$, $p_0 = 1$ (bottom right). All curves terminate at the stellar exterior, $u = U$.

If $b_s \neq 0$, then the relation $a_A = \partial \log M / \partial \phi_\infty$ [2] can be used to simplify $\mathcal{M}_{(1)}$:

$$\begin{aligned}
\mathcal{M}_{(1)} = & \frac{9\sqrt{3}}{2b_s} \arccos\left(\frac{1+p_0}{1+3p_0}\right) - \frac{\sqrt{3p_0(1+2p_0)}(41p_0^2 + 34p_0 + 9)}{b_s(1+p_0)(1+3p_0)^2} \\
& - \frac{96(1+p_0)\sqrt{3p_0^3(1+2p_0)^3}}{b_s(1+3p_0)^4} \dot{\varphi}_{(0)}(1+b_s\varphi_{(0)}) + \frac{8\sqrt{3p_0(1+2p_0)}}{1+p_0} \mu_{(1)} \\
& + \frac{24(1+p_0)\sqrt{3p_0(1+2p_0)}}{(1+3p_0)^2} p_{(1)}. \tag{5.62}
\end{aligned}$$

5.4 Comparing perturbative solutions with numerics

Part of the utility of analyzing the incompressible star in such detail is that such explicit expressions for the perturbative solutions allow a detailed comparison with direct numerical integrations. This helps indicate the domain of validity of the perturbative results.

First, we look at the profiles for the physical variables $\mu(u)$, $p(u)$, and $\varphi(u)$ across the interior of the star. The quantities μ , p and φ are respectively plotted versus u in Figures (8), (9) and (10), for $a_0^2 = 0.1$ and several choices for b_s , and p_0 . The line labelled “Zeroth Order” plots the zeroeth-order result, *e.g.* $\mu_{(0)}$, while the line labelled “First Order” includes also the first correction, *e.g.* $\mu_{(0)} + a_0^2\mu_{(1)}$. Notice that the curves all lie close to one other for small u , but begin to separate at the stellar exterior, $u \rightarrow U$. Furthermore, the separation is

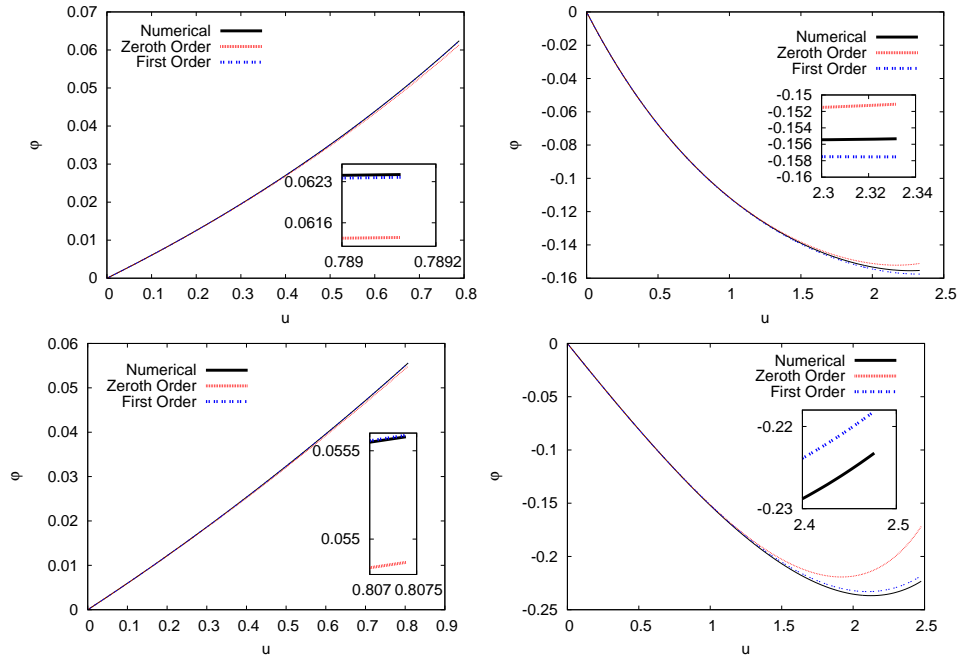


Figure 10: Comparison of φ vs u calculated perturbatively and numerically for an incompressible star in quasi-Brans/Dicke theory with $a_0^2 = 0.1$ and $b_s = 4$, $p_0 = 0.1$ (top left); $b_s = 4$, $p_0 = 1$ (top right); $b_s = -4$, $p_0 = 0.1$ (bottom left); and $b_s = -4$, $p_0 = 1$ (bottom right). All curves terminate at the stellar exterior, $u = U$.

largest for the more relativistic stars, for which p_0 is larger. However in all cases displayed the perturbative results capture the full numerics quite well throughout the entire star, with the strongest deviations happening for $\varphi(u)$ when $b_s < 0$.

Of more practical interest is a similar comparison of the accuracy of the perturbative expressions for plots that directly relate observable quantities to one another, such as plots of a_A vs s . Examples of these are given in figures (11), which give s , $\mathcal{A} = a_A/a_0$, $\mathcal{F} = (\phi_\infty - \phi_0)/a_0$ and \mathcal{M} as functions of the central pressure, $p_0 = P_0/\rho_0$ for the special case of Brans-Dicke theory ($b_s = 0$) with $a_0^2 = a_s^2 = 0.1$. These again show good agreement between perturbative and numerical calculations, with the biggest deviations arising in the most relativistic settings (largest p_0).

6. Conclusions

In this paper we set up the equations of stellar structure, with the stellar interior modeled as a spherically symmetric, static fluid, and with gravity described by a scalar-tensor theory with a single light scalar coupling to matter only through its coupling to a Jordan frame metric. For practical reasons, and for the purposes of making contact with earlier workers, we focus on the special case where the scalar-matter coupling function does not vary strongly with the field, $a(\phi) \simeq a_s + b_s\phi$.

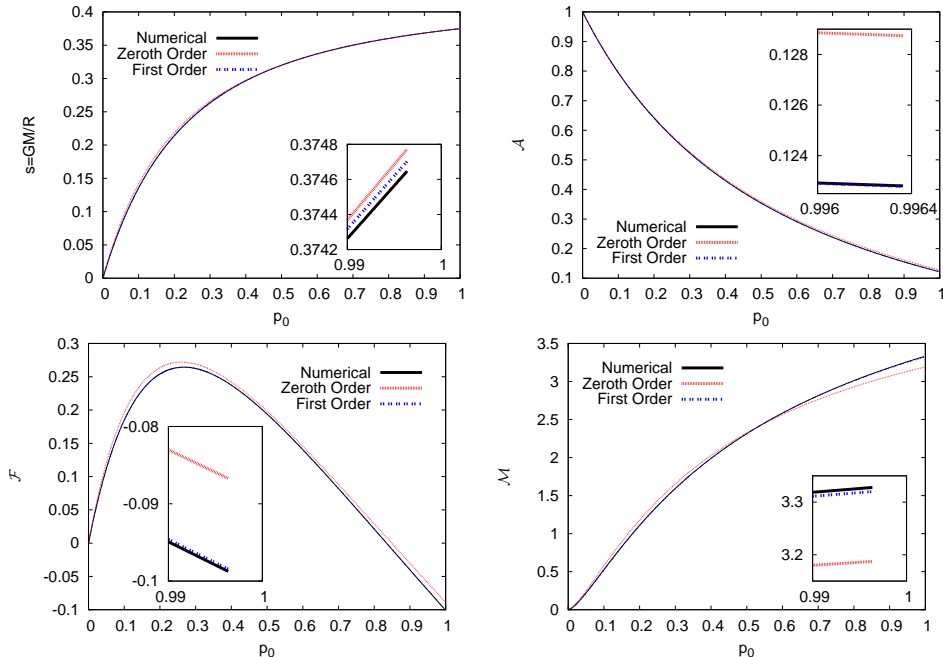


Figure 11: Comparison of physical quantities as functions of central pressure, $p_0 = P_0/\rho_0$, calculated perturbatively and numerically for an incompressible star in Brans-Dicke theory ($b_s = 0$) with $a_s^2 = 0.1$. The plots show compactness, s (top left); external coupling, $\mathcal{A} = a_A/a_s = Q/Ma_s$, (top right); $\mathcal{F} = (\phi_\infty - \phi_0)/a_s$ (bottom left); and \mathcal{M} (bottom right).

We seek solutions to these equations, for a variety of equations of state, in the special case where the scalar-matter coupling at the stellar center is small, $a_0^2 = a^2(\phi_0) \ll 1$. We obtain solutions as perturbations to those of General Relativity. By comparing these solutions with explicit numerical integration we verify that the perturbative approximation works well throughout most of the star.

These perturbative solutions have the merit of being very simple to integrate numerically, and of allowing analytic solutions for some choices of equation of state. This is very convenient for efficiently exploring different choices for the scalar properties, and scalar-matter couplings.

We use these solutions to compute the form of the observable relations that are imposed among the external properties of the stars by the condition that they match continuously to the stellar interior. There are two such relations among the four external variables, M , R , Q and ϕ_∞ , and our semi-analytic approach allows a simple exposition of how these relations depend on scalar properties. These properties ultimately underly any tests of scalar-tensor theories using astrophysical systems, such as binary pulsars.

Finally, these methods are applied to the illustrative case of an incompressible star, for which the density is constant. In this case the solutions generated by the a_0 expansion may be found analytically, making the comparisons with numerical results particularly simple. Again we find that the perturbative expressions agree well with the solutions obtained by numerical integration.

Acknowledgements

We thank Nemanja Kaloper and Maxim Pospelov for useful discussions. This research was supported in part by funds from the Natural Sciences and Engineering Research Council (NSERC) of Canada. Research at the Perimeter Institute is supported in part by the Government of Canada through Industry Canada, and by the Province of Ontario through the Ministry of Research and Information (MRI).

A. Expansions for large b_s

This appendix evaluates the large- b_s expansion for the properties of incompressible stars.

The coefficients c_r of the power series (5.37) can be written explicitly as

$$c_r = \sum_{i=0}^r a_i^{(r)} b_s^i, \quad (\text{A.1})$$

where $a_i^{(r)}$ is a polynomial in p_0 of degree r . It follows from equation (5.41) that $a_r^{(r)}$ satisfy a two-term recurrence relation, which can be solved explicitly, giving

$$a_r^{(r)} = \frac{[6(1-3p_0)]^r}{(2r+1)!}. \quad (\text{A.2})$$

The coefficients $a_0^{(r)}$ vanish for $r \geq 1$, and the remaining coefficients are given by

$$a_{r-k}^{(r)} = \frac{r! \cdot [6(1-3p_0)]^{r-2k}}{(2r+1)!(r-k-1)!} \sum_{j=0}^{2k-1} P_{k,j}(p_0) r^j, \quad (k \geq 1, r-k \geq 1) \quad (\text{A.3})$$

where $P_{k,j}$ is a polynomial of degree $2k$ with rational coefficients. The first of these polynomials are given by

$$P_{1,0}(p_0) = 2(63p_0^2 - 18p_0 + 7), \quad (\text{A.4})$$

$$P_{1,1}(p_0) = 8(9p_0^2 + 9p_0 + 4), \quad (\text{A.5})$$

$$P_{2,0}(p_0) = \frac{6}{5}(-3321p_0^4 + 2916p_0^3 + 6426p_0^2 + 4644p_0 + 679), \quad (\text{A.6})$$

$$P_{2,1}(p_0) = \frac{2}{5}(5913p_0^4 - 21708p_0^3 + 29502p_0^2 + 17028p_0 + 2593), \quad (\text{A.7})$$

$$P_{2,2}(p_0) = \frac{48}{5}(729p_0^4 - 729p_0^3 - 1989p_0^2 - 1251p_0 - 176), \quad (\text{A.8})$$

$$P_{2,3}(p_0) = 32(9p_0^2 + 9p_0 + 4)^2, \quad (\text{A.9})$$

and the higher ones can be computed from the relation

$$\begin{aligned}
& \frac{r!}{12(r-l-1)!} \sum_{i=0}^{2l-1} P_{l,i}(p_0) r^i = \\
& = 24 \sum_{j=l}^{r-1} \frac{(2j+1)(j+2)(1+3p_0)(1-3p_0)^2 j!}{(j-l)!} \sum_{i=0}^{2l-5} P_{l-2,i}(p_0) (j-1)^{i+1} \\
& \quad + \sum_{j=l}^{r-1} \frac{(1-9p_0-6jp_0)(1-3p_0)jj!}{(j-l)!} \sum_{i=0}^{2l-3} P_{l-1,i}(p_0) j^i \\
& \quad + 4 \sum_{j=l+1}^{r-1} \frac{(2j+1)(1+3p_0)j!}{(j-l-1)!} \sum_{i=0}^{2l-3} P_{l-1,i}(p_0) (j-1)^i, \tag{A.10}
\end{aligned}$$

which holds for $l \geq 3$ and $r \geq l+1$.

From the identities [67]

$$\sum_{k=0}^n (-1)^k \binom{n}{k} (k+a)^n = (-1)^n n!, \quad (n \geq 0, a \in \mathbb{R}) \tag{A.11}$$

$$\sum_{k=0}^N (-1)^k \binom{N}{k} (k+a)^{n-1} = 0, \quad (N \geq n \geq 1, a \in \mathbb{R}) \tag{A.12}$$

it follows that

$$P_{k,2k-1}(p_0) = \frac{[8(9p_0^2 + 9p_0 + 4)]^k}{k!}. \quad (k \geq 1) \tag{A.13}$$

Write

$$P_{k,j}(p_0) = \sum_{l=0}^{2k} q_{k,j}^{(l)} p_0^l. \tag{A.14}$$

By means of telescopic summation, the identity (A.10) can be used to derive recurrence relations for the coefficients $q_{k,j}^{(l)}$. In general, these recurrence relations are very complicated, but for $l = 2k$, they are particularly simple:

$$(k+1)q_{k,0}^{(2k)} + \sum_{i=1}^{2k-1} q_{k,i}^{(2k)} = 0, \tag{A.15}$$

$$(k+2)q_{k,1}^{(2k)} + \sum_{i=2}^{2k-1} (i+1)q_{k,i}^{(2k)} = 324q_{k-1,0}^{(2k-2)}, \tag{A.16}$$

$$(k+j+1)q_{k,j}^{(2k)} + \sum_{i=j+1}^{2k-1} \binom{i+1}{j} q_{k,i}^{(2k)} = 216q_{k-1,j-2}^{(2k-2)} + 324q_{k-1,j-1}^{(2k-2)}, \tag{A.17}$$

where $k \geq 2$ and $2 \leq j \leq 2k-2$.

Now, $\varphi_{(0)}$ can be expanded in the form

$$\begin{aligned}
\varphi_{(0)}(z) &= \frac{1}{b_s} \left[(a_1^{(1)}b_s + a_0^{(1)})z + (a_2^{(2)}b_s^2 + a_1^{(2)}b_s + a_0^{(2)})z^2 \right. \\
&\quad \left. + (a_3^{(3)}b_s^3 + a_2^{(3)}b_s^2 + a_1^{(3)}b_s + a_0^{(3)})z^3 + \dots \right] \\
&= \frac{1}{b_s} \left(a_1^{(1)}(b_s z) + a_2^{(2)}(b_s z)^2 + a_3^{(3)}(b_s z)^3 + \dots \right) \\
&\quad + \frac{1}{b_s^2} \left(a_0^{(1)}(b_s z) + a_1^{(2)}(b_s z)^2 + a_2^{(3)}(b_s z)^3 + \dots \right) + \dots \\
&\equiv \frac{\varphi_{(0)}^{(1)}(b_s z)}{b_s} + \frac{\varphi_{(0)}^{(2)}(b_s z)}{b_s^2} + \dots .
\end{aligned} \tag{A.18}$$

It follows from equations (A.2) and (A.3) that

$$\varphi_{(0)}^{(1)}(b_s z) = \frac{\sinh \sqrt{t}}{\sqrt{t}} - 1, \tag{A.19}$$

$$\varphi_{(k+1)}^{(0)}(b_s z) = \frac{1}{[6(1-3p_0)]^{2k}} \sum_{j=0}^{2k-1} P_{k,j}(p_0) f_{k,j}(t), \quad (k \geq 1) \tag{A.20}$$

where

$$\begin{aligned}
f_{k,j}(t) &= \sum_{r=k+1}^{\infty} \frac{r! \cdot t^r r^j}{(2r+1)!(r-k-1)!} \\
&= \left(t \frac{d}{dt} \right)^j \left(-\frac{i\sqrt{t}}{2} \right)^{k+1} j_{k+1}(i\sqrt{t}),
\end{aligned} \tag{A.21}$$

where

$$j_n(x) = \sqrt{\frac{\pi}{2x}} J_{n+\frac{1}{2}}(x) = (-x)^n \left(\frac{1}{x} \frac{d}{dx} \right)^n \frac{\sin x}{x} \tag{A.22}$$

are the spherical Bessel functions, and $t = 6b_s(1-3p_0)z = 3b_s(1-3p_0)(1 - \sqrt{1-u/3})$.

The spherical Bessel functions satisfy the recursion relations

$$\begin{aligned}
xj_{l-1}(x) + xj_{l+1}(x) &= (2l+1)j_l(x), \\
lj_{l-1}(x) - (l+1)j_{l+1}(x) &= (2l+1)j'_l(x).
\end{aligned} \tag{A.23}$$

Therefore, the $f_{k,j}$ satisfy the recursion relations

$$\begin{aligned}
f_{k,1} &= f_{k+1,0} + (k+1)f_{k,0}, \\
tf_{k-1,0} - 4f_{k+1,0} &= 2(2k+3)f_{k,0}.
\end{aligned} \tag{A.24}$$

The first of these relations can be used to write $f_{k,j}$ explicitly in terms of $f_{l,0}$:

$$f_{k,j} = f_{k+j,0} + \sum_{m=1}^j \left[\sum_{l_1, \dots, l_m=1}^{\sim j-m+1} (k+l_1) \dots (k+l_m) \right] f_{k+j-m,0}, \quad (\text{A.25})$$

for $j \geq 1$. The tilde on the sum means that all numerical factors which come from overcounting should be deleted. For example,

$$\sum_{l_1, l_2=1}^{\sim 2} (k+l_1)(k+l_2) = (k+1)^2 + (k+1)(k+2) + (k+2)^2. \quad (\text{A.26})$$

Equations (5.10)-(5.11) then become

$$\mathcal{A}_{(0)} = \frac{1+p_0}{p_0} \left\{ \frac{1}{2b_s} \left(\cosh \sqrt{T} - \frac{\sinh \sqrt{T}}{\sqrt{T}} \right) + \sum_{k=1}^{\infty} \sum_{j=0}^{2k-1} \frac{P_{k,j}(p_0) f_{k,j+1}(T)}{b_s^{k+1} [6(1-3p_0)]^{2k}} \right\}, \quad (\text{A.27})$$

$$\begin{aligned} \mathcal{F}_{(0)} = & \frac{1}{b_s} \left(\left[1 + \frac{1+p_0}{2p_0} L \right] \frac{\sinh \sqrt{T}}{\sqrt{T}} - \frac{1+p_0}{2p_0} L \cosh \sqrt{T} - 1 \right) \\ & + \sum_{k=1}^{\infty} \sum_{j=0}^{2k-1} \left(f_{k,j}(T) - \frac{1+p_0}{p_0} L f_{k,j+1}(T) \right) \frac{P_{k,j}(p_0)}{b_s^{k+1} [6(1-3p_0)]^{2k}}, \end{aligned} \quad (\text{A.28})$$

where $T = 6b_s p_0 (1 - 3p_0) / (1 + 3p_0)$ is the value of the variable t corresponding to $u = U$, and $L = \log(1 + p_0) - \log(1 + 3p_0)$. If $b_s > 0$, then $T \leq (6 - 4\sqrt{2})b_s \sim 0.34b_s$. If $b_s < 0$, then $T \geq -(6 - 4\sqrt{2})|b_s| \sim -0.34|b_s|$. The above expressions (A.27) and (A.28) can be used to calculate the second constraint (4.11).

These perturbative solutions have a limited regime of applicability. They break down as $b_s \rightarrow 0$, because the $1/b_s$ expansion fails. But they also break down at the onset of spontaneous scalarization.

References

- [1] T. Chiba, T. Harada, and K. Nakao, *Prog. Theor. Phys. Suppl.* **128** (1997) 335.
- [2] T. Damour and G. Esposito-Farèse, *Class. and Quant. Grav.* **9** (1992) 2093.
- [3] Y. Fujii and K. Maeda, *The Scalar-Tensor Theory of Gravitation*, Cambridge University Press 2003.
- [4] V. Faraoni, *Cosmology in Scalar-Tensor Gravity*, Kluwer Academic Publishers 2004.
- [5] T. Singh and L. N. Rai, *Gen. Rel. Grav.* **15** (1983) 875.
- [6] C. H. Brans, [arXiv:gr-qc/0506063].
- [7] S. Weinberg, *Phys. Rev. Lett.* **29** (1972) 1698.
- [8] C. P. Burgess, A. Maharana and F. Quevedo, arXiv:1005.1199 [hep-th].
- [9] C. M. Will, *Living Rev. Rel.* **9** (2005) 3 [arXiv:gr-qc/0510072].

- [10] G. Esposito-Farèse, AIP Conf. Proc. **736** (2004) 35 [arXiv:gr-qc/0409081].
- [11] T. Damour and G. Esposito-Farèse, Phys. Rev. D **54** (1996) 1474 [arXiv:gr-qc/9602056];
T. Damour, arXiv:0704.0749 [gr-qc];
G. Esposito-Farèse, [arXiv:gr-qc/0402007].
- [12] T. Damour and G. Esposito-Farèse, Phys. Rev. D **58** (1998) 042001 [arXiv:gr-qc/9803031].
- [13] N. D. R. Bhat, M. Bailes and J. P. W. Verbiest, Phys. Rev. D **77** (2008) 124017
[arXiv:0804.0956 [astro-ph]];
K. Lazaridis *et al.*, Mon. Not. R. Astron. Soc. **400** (2009) 805 [arXiv:0908.0285 [astro-ph.GA]].
- [14] S. DeDeo and D. Psaltis, Phys. Rev. Lett. **90** (2003) 141101 [arXiv:astro-ph/0302095] ;
S. DeDeo and D. Psaltis, Bull. Am. Astron. Soc. **36** (2004) 944 [arXiv:astro-ph/0405067];
D. Psaltis, arXiv:0806.1531 [astro-ph].
- [15] O. G. Benvenuto, L. G. Althaus, and D. F. Torres, Mon. Not. R. Astron. Soc. **305** (1999) 905.
- [16] H. Sotani and K. D. Kokkotas, Phys. Rev. D **70** (2004) 084026 [arXiv:gr-qc/0409066];
H. Sotani and K. D. Kokkotas, Phys. Rev. D **71** (2005) 124038 [arXiv:gr-qc/0506060].
- [17] D. Psaltis, Astrophys. J. **688** (2008) 1282 [arXiv:astro-ph/0501234].
- [18] T. Damour and G. Esposito-Farèse, Phys. Rev. Lett. **70** (1993) 2220.
- [19] H. A. Buchdahl, Phys. Rev. **116** (1959) 1027.
- [20] S. Weinberg, *Gravitation and Cosmology*, John Wiley & Sons 1972.
- [21] C. W. Misner, K. S. Thorne, and J. A. Wheeler, *Gravitation*, W. H. Freeman and Company 1973.
- [22] C. Brans and R. H. Dicke, Phys. Rev. **124** (1961) 925;
R. H. Dicke, Phys. Rev. **125** (1962) 2163;
C. Brans, Phys. Rev. **125** (1962) 2194.
- [23] P. G. Bergmann, Int. J. Theor. Phys. **1** (1968) 25;
R. V. Wagoner, Phys. Rev. D **1** (1970) 3209;
K. Nordtvedt, Astrophys. J. **161** (1970) 1059.
- [24] T. Damour and A. M. Polyakov, Gen. Rel. Grav. **26** (1994) 1171 [arXiv:gr-qc/9411069];
Nucl. Phys. B **423** (1994) 532 [arXiv:hep-th/9401069].
- [25] A. Albrecht, C. P. Burgess, F. Ravndal and C. Skordis, Phys. Rev. D **65** (2002) 123507
[arXiv:astro-ph/0107573];
K. Kainulainen and D. Sunhede, Phys. Rev. D **73** (2006) 083510 [arXiv:astro-ph/0412609].
- [26] D. F. Mota and J. D. Barrow, Phys. Lett. **B581** (2004) 141 [arXiv:astro-ph/0306047].
- [27] J. Khoury and A. Weltman, Phys. Rev. Lett. **93** (2004) 171104 [arXiv:astro-ph/0309300].
- [28] K. A. Olive and M. Pospelov, Phys. Rev. D **77** (2008) 043524 [arXiv:0709.3825 [hep-ph]].

- [29] J.H. Taylor, Rev. Mod. Phys. **66** (1994) 711;
E.S. Phinney and S.R. Kulkarni, Ann. Rev. Astron. Astrophys. **32** (1994) 591.
- [30] I. H. Stairs, Living Rev. Rel. **6** (2003) 5 [arXiv:astro-ph/0307536];
R. P. Breton *et al.*, AIP Conf. Proc. **983** (2008) 469.
- [31] J. M. Weisberg and J. H. Taylor, ASP Conf. Ser. **328** (2005) 25 [arXiv:astro-ph/0407149].
- [32] T. Harada, Prog. Theor. Phys. **98** (1997) 359 [arXiv:gr-qc/9706014];
T. Harada, Phys. Rev. D **57** (1998) 4802 [arXiv:gr-qc/9801049].
- [33] J. Novak, Phys. Rev. D **57** (1998) 4789;
J. Novak, Phys. Rev. D **58** (1998) 064019 [arXiv:gr-qc/9806022];
J. Novak and J. M. Ibáñez, Astrophys. J. **533** (2000) 392;
M. Alcubierre, J. C. Degollado, D. Nunez, M. Ruiz and M. Salgado, Phys. Rev. D **81** (2010) 124018 [arXiv:1003.4767 [gr-qc]].
- [34] A. Salmona, Phys. Rev. **154** (1967) 1218.
- [35] Y. Nutku Astrophys. J. **155** (1969) 999.
- [36] G. S. Saakyan and M. A. Mnatsakanyan, Astrophysics **3** (1967) 311;
G. S. Saakyan and M. A. Mnatsakanyan, Astrophysics **4** (1968) 567;
R. M. Avakyan and M. A. Mnatsakanyan, Astrophysics **5** (1969) 169;
G. S. Saakyan and M. A. Mnatsakanyan, Astrophysics **5** (1969) 555.
- [37] T. Matsuda, Prog. Theor. Phys. **48** (1972) 341.
- [38] K. Yokoi, Prog. Theor. Phys. **48** (1972) 1760.
- [39] H. Heintzmann, W. Hillebrandt, M. F. El Eid, and E. R. Hilf, Z. Naturforsch. **29a** (1974) 933.
- [40] W. Hillebrandt and H. Heintzmann, Gen. Rel. Grav. **5** (1974) 663.
- [41] V. I. Reizlin, Sov. J. Phys. **19** (1976) 1403.
- [42] R. A. Saenz, Astrophys. J. **212** (1977) 816.
- [43] W. F. Bruckman and E. Kazes, Phys. Rev. D **16** (1977) 261;
W. F. Bruckman and E. Kazes, Phys. Rev. D **16** (1977) 269.
- [44] A. Banerjee and D. Bhattacharya, J. Math. Phys. **20** (1979) 1908;
A. Banerjee and N. O. Santos, Int. J. Theor. Phys. **20** (1981) 315.
- [45] R. M. Avakyan, G. G. Arutyunyan, and V. V. Papoyan, Astrophysics **33** (1991) 338.
- [46] H. W. Zaglauer, Astrophys. J. **393** (1992) 685.
- [47] W. F. Bruckman and E. S. Velázquez, Gen. Rel. Grav. **25** (1993) 901.
- [48] M. Salgado, D. Sudarsky and U. Nucamendi, Phys. Rev. D **58** (1998) 124003
[arXiv:gr-qc/9806070].
- [49] A. W. Whinnett Phys. Rev. D **61** (2000) 124014 arXiv:gr-qc/9911052.

- [50] S. M. Kozyrev, arXiv:gr-qc/0207039.
- [51] A. W. Whinnett and D. F. Torres, *Astrophys. J.* **603** (2004) L133 [arXiv:astro-ph/0401521].
- [52] M. Salgado, D. Sudarsky and U. Nucamendi, *Phys. Rev. D* **70** (2004) 084027 [arXiv:gr-qc/0402126].
- [53] S. S. Yazadjiev, *Phys. Rev. D* **69** (2004) 127501 [arXiv:gr-qc/0312019];
S. S. Yazadjiev, *Mod. Phys. Lett. A* **20** (2005) 821 [arXiv:gr-qc/0411132]
- [54] J. P. Crawford and D. Kazanas, *Astrophys. J.* **701** (2009) 1701.
- [55] O. Heckmann, P. Jordan, and R. Fricke, *Astroph. Z* **28** (1951) 113.
- [56] R. Arnowitt, S. Deser, and C. Misner, *Phys. Rev.* **122** (1961) 997.
- [57] T. Damour and G. Esposito-Farese, *Phys. Rev. D* **53** (1996) 5541 [arXiv:gr-qc/9506063].
- [58] T. Tsuchida, G. Kawamura and K. Watanabe, *Prog. Theor. Phys.* **100** (1998) 291 [arXiv:gr-qc/9802049].
- [59] R. Ruffini and J. A. Wheeler, *Phys. Today* **24** (1971) 30.
- [60] J. E. Chase, *Commun. Math. Phys.* **19** (1970) 276,
J. D. Bekenstein, *Phys. Rev. Lett.* **28** (1972) 452,
C. Teitelboim, *Lett. Nuov. Cim.* **3** (1972) 326,
S. W. Hawking, *Commun. Math. Phys.* **25** (1972) 167.
- [61] M. Camenzind, *Compact Objects in Astrophysics*, Springer-Verlag 2007.
- [62] S. Chandrasekhar, *Astrophys. J.* **74** (1931) 81.
- [63] C. J. Hansen and S. D. Kawaler, *Stellar Interiors*, Springer-Verlag 1994.
- [64] S. Chandrasekhar, *An Introduction to the Study of Stellar Structure*, Dover Publications 1958.
- [65] K. Schwarzschild, *Sitzungsberichte Preuss. Akad. Wiss.* (1916) 424.
- [66] S. Carroll, *Spacetime and Geometry: An Introduction to General Relativity*, Benjamin Cummings (2003).
- [67] I. S. Gradshteyn and I. M. Ryzhik, *Table of Integrals, Series, and Products*, Elsevier 2007.
- [68] A. Ronveaux, *Heun's Differential Equations*, Clarendon Press 1999.
- [69] A. W. Hendry, *Am. J. Phys.* **61** (1993) 906.

Symbol	Definition	Equation	Meaning
G		(2.1)	Einstein-frame gravitational constant
$g_{\mu\nu}$		(2.1)	Einstein-frame metric
ϕ		(2.1)	Einstein-frame scalar field
$\tilde{g}_{\mu\nu}$	$A^2(\phi)g_{\mu\nu}$	(2.1)	Jordan-frame metric
$a(\phi)$	$d(\log A(\phi))/d\phi$	(2.3)	Scalar-matter coupling function
$b(\phi)$	$da(\phi)/d\phi$	(2.6)	Derivative of scalar-matter coupling function
a_s, b_s	$a(\phi) = a_s + b_s\phi$	(2.8)	Parameters of the quasi-Brans/Dicke model
a_0	$a(\phi_0)$	(3.39)	Scalar-matter coupling in centre of star
φ	$(\phi - \phi_0)/a(\phi_0)$	(3.38)	Shifted and scaled Einstein-frame scalar field
r		(3.1)	Schwarzschild coordinate radial variable
u	$8\pi G\rho_0 A^4(\phi_0)r^2$	(3.38)	Radial variable
z	$(1 - \sqrt{1 - u/3})/2$	(5.31)	Dimensionless radial variable for constant-density stars
t	$6b_s(1 - 3p_0)z$	(A.19)	Dimensionless radial variable for constant-density stars
p_0	P_0/ρ_0	(3.12)	Pressure-to-density ratio in centre of star
$\mu(r)$	$(1 - g^{rr})/2$	(3.1)	Related to rr component of Einstein-frame metric
$\nu(r)$	$\log(-g_{tt})$	(3.1)	Related to tt component of Einstein-frame metric
$n(r)$		(3.31)	Baryon number density
R	$P(R) = 0$	(3.25)	Schwarzschild coordinate radius of star
U	$8\pi G\rho_0 A^4(\phi_0)R^2$		Value of u corresponding to $r = R$
T	$6b_s p_0(1 - 3p_0)/(1 + 3p_0)$		Value of t corresponding to $r = R$
M	$g_{tt} = -1 + 2GM/r + \dots$	(3.25)	ADM Mass of Einstein-frame metric
s	GM/R		Self-gravity, or compactness, of star
M_B		(3.31)	Baryonic mass of star
Q	$\phi = \phi_\infty - GQ/r + \dots$	(3.26)	Scalar charge of star
a_A	Q/M		Effective scalar-matter coupling of star
\mathcal{A}	$a_A/a(\phi_0)$		Rescaled effective scalar-matter coupling of star
ϕ_∞	$\phi(r = \infty)$	(3.27)	Asymptotic value of Einstein-frame scalar field
ϕ_0	$\phi(r = 0)$	(3.12)	Value of Einstein-frame scalar field in centre of star
\mathcal{F}	$(\phi_\infty - \phi_0)/a(\phi_0)$		Change in ϕ
P		(3.4)	Jordan-frame pressure
p	P/ρ_0	(3.8)	Rescaled Jordan-frame pressure
$\varrho(p; p_0)$	ρ/ρ_0	(3.8)	Equation of state
ρ		(3.4)	Jordan-frame mass-energy density

Table 1: Table of Notation